A statistical study on the peak and fluence spectra of Solar Energetic Particles observed over 4 solar cycles

YUBAO WANG [1] AND JINGNAN GUO [1,2,3]

[1]*Deep Space Exploration Laboratory/School of Earth and Space Sciences, University of Science and Technology of China, Hefei 230026, China*

[2]*CAS Center for Excellence in Comparative Planetology, University of Science and Technology of China, Hefei 230026, China*

[3]*Collaborative Innovation Center of Astronautical Science and Technology, Harbin 150001, China*

ABSTRACT

Solar energetic particles (SEPs) are an important space radiation source, especially for the space weather environment in the inner heliosphere. The energy spectrum of SEP events is crucial both for evaluating their radiation effects and for understanding their acceleration process at the source region and their propagation mechanism. In this work, we investigate the properties of the SEP peak flux spectra and the fluence spectra and their potential formation mechanisms using statistical methods. We aim to advance our understanding of both SEPs' acceleration and propagation mechanisms. Employing the dataset of ESA's Solar Energetic Particle Environment Modelling (SEPEM) program, we have obtained and fitted the peak-flux and fluence proton spectra of more than a hundred SEP events from 1974 to 2018. We analyzed the relationship among the solar activity, X-ray peak intensity of solar flares and the SEP spectral parameters. Based on the assumption that the initial spectrum of accelerated SEPs generally has a power-law distribution and also the diffusion coefficient has a power-law dependence on particle energy, we can assess both the source and propagation properties using the observed SEP event peak flux and fluence energy spectra. We confirm that SEPs' spectral properties are influenced by the solar source and the interplanetary conditions and their transportation process can be influenced by different phases of solar cycle. This study provides an observational perspective on the double power-law spectral characteristics of the SEP energy spectra, showing their correlation with the adiabatic cooling and diffusion processes during the particle propagation from the Sun to the observer. This contributes to a deeper understanding of the acceleration and propagation of SEP events, in particular the possible origins of the double-power law.

Keywords: Sun: particle emission–Sun: activity–Sun: flares–sunspots–Diffusion

1. INTRODUCTION

Corresponding author: Jingnan Guo
jnguo@ustc.edu.cn

In order to carry out space exploration activities, we need to have a clear understanding of the radiation environment in space. The energy spectrum of high-energy particles in space is a direct input for evaluating radiation dose. As the ultimate source, the Sun not only releases high-energy charged particles, but also significantly affects the propagation of particles. So the observed energy spectrum varies due to the different properties of particle acceleration and propagation processes. Various studies have attempted to use the observed data and existing knowledge to reconstruct these two aspects of information (see, e.g., Klein & Dalla 2017, and references therein).

Typically, there are two mechanisms that contribute to the acceleration of charged particles (Reames 1999, 2013): magnetic reconnection acceleration associated with flares and shock wave acceleration associated with Coronal Mass Ejections (CMEs). Ideally, we may be able to distinguish different acceleration processes by comparing the composition and state of particles in the chromosphere and corona, such as proton-to-electron ratios, ^{3}He compositions, and ion charge states (Mason 2007; Klein & Dalla 2017). But due to the fact that a SEP event is often associated with the onsets of both a solar flare and a CME, it is difficult to distinguish the role of the two types of acceleration processes. Furthermore, tracking the source of SEP events becomes more challenging when considering the propagation process of particles (see, e.g., Guo et al. 2024, and references therein).

Once SEPs are released into interplanetary space, their propagation can be theoretically described by the Fokker-Planck equation below (Parker 1965):

$$\frac{\partial U}{\partial t} = -\frac{V_{sw}}{r^2}\frac{\partial}{\partial r}\left(r^2 U\right) + \frac{2V_{sw}}{3r}\frac{\partial}{\partial E}[UEn(E)] + \frac{1}{r^2}\frac{\partial}{\partial r}\left(\kappa r^2 \frac{\partial U}{\partial r}\right);$$ (1)

$$n(E) = \frac{pdE}{Edp} = \frac{E + 2m_0 c^2}{E + m_0 c^2}.$$ (2)

Here $U(r, E, t)$ represents the probability distribution over kinetic energy E for location r and time t; V_{sw} is solar wind speed; κ is diffusion coefficient; and m_0 is rest mass of the particle. $n(E)$ represents the normalized conversion coefficient between particle momentum p and kinetic energy E. For relativistic particles, $n(E) \approx 1$, and for non-relativistic particles, $n(E) \approx 2$. The terms on the right-hand side of Eq. 1 originate from three particle transport mechanisms: convection, adiabatic cooling, and diffusion. Each of these transport mechanisms may modify the original acceleration characteristics of energetic particles.

In this study, we focus on the properties of SEP proton energy spectra and statistically investigate the correlation between solar activity index and the properties of SEP events. We aim to extract information about the acceleration and propagation processes of SEPs combining analytical descriptions of particle propagation and parameters obtained from observations. Analytical details about SEP energy spectra will be introduced in Sect. 2. The dataset, SEP event list, and fitting method will be introduced in Sect. 3. Subsequently, we will examine the distributions of SEP proton energy spectra parameters, the relationships between integral fluence spectra and peak flux spectra, and how they change with the solar cycle in Sect. 4. The results and conclusions will be summarized in Sect. 5.

2. ANALYTICAL DESCRIPTIONS OF SEP ENERGY SPECTRA

The SEP energy spectrum is the flux distribution of SEPs versus the particle energy, which is determined by both the acceleration process and transport effects. The SEP spectrum can be directly

measured by high-energy particle detectors in space, and some large SEP events can also be indirectly recorded by ground neutron detectors or muon detectors when the secondary particles have energy high enough to reach the surface of Earth, also known as Ground-Level enhancement (GLE) events (see, e.g., Sect. 3 of Guo et al. 2024, and references therein). By adopting different integration time windows, we can study the event energy spectrum and its time evolution. The most-frequently referred one is the integrated fluence spectrum of the entire event. This spectrum accumulates the flux of particles over different energies from the beginning to the end of the event, and it is crucial for evaluating the total radiation effect of the event. Another important one is the time-of-maximum (TOM) energy spectrum or peak flux spectrum formed by the maximum flux at each energy bin. This method can minimize the impact of solar wind on energetic particle propagation processes, such as diffusion, convection, and velocity dispersion effects, allowing for a more reasonable estimation of the energy spectrum of the source region (Van Hollebeke 1975).

2.1. *Integral fluence spectra*

Previous researchers have proposed multiple functions to describe the integral fluence spectra of SEP events. The most commonly used functions are the single power law with an exponential rollover function (e.g., Tylka 2001) and the double power law function (e.g., Mewaldt et al. 2012; Osku Raukunen et al. 2018). The latter is also called the Band function, which was originally proposed for fitting γ-ray burst spectra (Band et al. 1993). It is confirmed that the Band formulation generally fits SEP integral fluence spectra better, especially for those large events (e.g., Mewaldt et al. 2005). Therefore we choose this function to fit SEP integral fluence spectra in this study. The Band function is given by:

$$\frac{dJ}{dE} = \begin{cases} CE^{\gamma_1} \exp\left(-E/E_0\right), \\ \quad \text{if } E < \left(\gamma_1 - \gamma_2\right) E_0; \\ CE^{\gamma_2} \left\{ \left[\left(\gamma_1 - \gamma_2\right) E_0\right]^{(\gamma_1 - \gamma_2)} \exp\left(\gamma_2 - \gamma_1\right) \right\}, \\ \quad \text{if } E \geq \left(\gamma_1 - \gamma_2\right) E_0. \end{cases} \tag{3}$$

Here C is an overall fluence normalization coefficient in the same units of dJ/dE; γ_1 is the power-law index at the low-energy range; γ_2 is the power-law index at the high-energy range; E is particle's kinetic energy as defined in Eq. 1; E and E_0 are measured in energy/nucleon; $(\gamma_1 - \gamma_2)E_0$ is break-point energy which separates the low-energy and high-energy ranges. Both the Band function and its first derivative are continuous at this break point. But we have to note that there is no clear physical meaning of the four free parameters of Band function, and this function is still a semi-phenomenological model. Due to the mixing of propagation effects such as diffusion and adiabatic cooling, it is difficult to directly obtain information on the source and propagation process of high-energy particles through the parameters defined by the integrated energy spectra. More discussions will be given in Sects. 4 and 5.

2.2. *Peak flux spectra*

When neglecting convection and adiabatic deceleration terms, the transportation of energetic particles can be treated as a process of simple time-dependent spherical diffusion from a point source. Then the time profile of a well-connected SEP event flux can be described by a simple function (e.g.,

Parker 1963):

$$j(p, r, t) = \frac{N_0(p)}{4\pi p^2} \frac{\exp\left(-r^2/4t\kappa(p)\right)}{2\sqrt{\pi}(t\kappa(p))^{3/2}}, \tag{4}$$

where $j(p,r,t)$ is particle's flux at location r, time t with momentum p, $\kappa(p)$ is energy-dependent diffusion coefficient, $N_0(p)$ is the number of particles per unit momentum released at the Sun. From Eq. 4, one can derive the peak flux spectrum for $t = t_{max} = r^2/(6\kappa(p))$, and one can see that peak flux spectrum has the same shape with the source spectrum (Forman et al. 1986):

$$j\left(p, r, t_{max}(r, p)\right) = \frac{(6/e)^{3/2}}{2\sqrt{\pi}r^3} \frac{N_0(p)}{4\pi p^2} \propto \frac{N_0(p)}{4\pi p^2}. \tag{5}$$

For the early stages of SEP events, the convective effect of particle propagation can be ignored compared to the diffusion effect (e.g., McCracken et al. 1971). When considering adiabatic deceleration and assuming a simple power-law diffusion coefficient

$$\kappa = \kappa_0 E^\alpha, \tag{6}$$

Kurt et al. (1981) estimated the particle's adiabatic energy loss ΔE as:

$$\Delta E = E_s - E = E_s - \left(E_s^\alpha - \frac{4}{9}\frac{V_{sw}r}{\kappa_0}\right)^{\frac{1}{\alpha}}, \tag{7}$$

where E_s is particle's kinetic energy directly being released at the Sun, E is particle's kinetic energy at location r, V_{sw} is solar wind speed, κ_0 is normalization coefficient in the same unit of diffusion coefficient κ, α is power-law index.

Previous studies have shown that for the two acceleration processes of SEPs, it is relatively reasonable to assume that the energy spectrum after acceleration follows a simple power-law (e.g., Jones & Ellison 1991; Dierckxsens et al. 2015; Fu et al. 2006):

$$j(E_s) = j_0 E_s^{-\gamma}, \tag{8}$$

where j_0 is normalization coefficient in the same units of particle's flux j, γ is the index of the power-law energy spectrum after acceleration. Based on the conservation of particle number and combined with Eq. 7, the particle energy spectrum at location r can be obtained as:

$$j(r, E) = j_0 \left(E^\alpha + \frac{4}{9}\frac{V_{sw}}{\kappa_0}r\right)^{-\frac{\gamma}{\alpha}}. \tag{9}$$

Figure 1 illustrates the impact of adiabatic energy loss on the spectrum as described by the above equation. We set an initial flux spectrum with parameters $j_0 = 10^8[\#/\text{cm}^2/\text{s}/\text{sr}/\text{MeV}]$, $\gamma = 4$, and a constant solar wind speed of V_{sw}=450 [km/s]. Panel a shows the peak flux spectra at 1 AU for different diffusion coefficient index α. Panel b shows the adiabatic energy loss of particles with a given initial energy corresponding to Panel a. Panel c shows the peak flux spectra at 1 AU with different diffusion normalization coefficient κ_0. Panel d shows the adiabatic energy loss of particles with a given initial energy corresponding to Panel c. Panel e shows the evolution of the peak flux

Table 1. Fourteen logarithmic energy bins of the third version of the SEPEM reference proton dataset.

Channel	Effective energy (Energy range) [MeV]	Channel	Effective energy (Energy range) [MeV]	Channel	Effective energy (Energy range) [MeV]
1	6.01(5.00-7.23)	6	38.03(31.62-45.73)	11	244.2(200.0-289.2)
2	8.70(7.23-10.46)	7	54.99(45.73-66.13)	12	347.8(289.2-418.3)
3	12.58(10.46-15.12)	8	79.53(66.13-95.64)	13	503.0(418.3-604.9)
4	18.18(15.12-21.87)	9	115.0(95.64-138.3)	14	727.4(604.9-874.7)
5	26.30(21.87-31.62)	10	166.3(138.3-200.0)		

spectrum at different heliocentric distance. Panel f shows the adiabatic energy loss corresponding to Panel e. From this graph, it can be seen that smaller diffusion coefficients, namely smaller κ_0 and α, will have a more pronounced adiabatic cooling effect on particles, especially for those with lower energy (less than tens of MeV). Additionally, as the propagation distance increases, the peak energy spectrum of SEP events will also become flatter.

3. SEPEM DATASET AND METHODS

The Solar Energetic Particle Environment Modelling (SEPEM) project is a WWW interface to SEP data together with a range of modelling tools and functionalities intended to support space mission design[1]. The system provides an implementation of several well-known modelling methodologies, built upon cleansed datasets. A large number of datasets have been combined into an SQL database for convenient access. SEPEM also affords the user increased flexibility in their analysis and enables the generation of mission-integrated fluence statistics, peak flux statistics, and other functionalities. Additionally, it integrates effect tools that calculate single-event upset rates and radiation doses for a variety of scenarios; the statistical methods can further be applied to these effect parameters.

In this work, we exploit the continuous and high-quality dataset and the long-term reference SEP event list to statistically study the properties of SEP spectra.

3.1. *SEPEM dataset*

The SEPEM reference proton dataset was originated from multiple spacecrafts and instruments[2], such as Space Environment Monitor (SEM) and Energetic Particles Sensor (EPS) of Geostationary Operational Environmental Satellite (GOES), and Goddard Medium Energy (GME) of Interplanetary Monitoring Platform 8 (IMP 8) satellite and further processed through correction, completion, cross-calibration, and energy rebinning (Crosby et al. 2015).

We selected the most up-to-date version (3rd version) of the SEPEM reference proton dataset for this study. This dataset includes proton flux data at 1AU with a time resolution of 5 minutes, spanning from July 1, 1974 to December 31, 2017. It also consists of 14 logarithmic energy bins ranging from 5 MeV to nearly 900 MeV, with Galaxy Cosmic Ray (GCR) background subtracted.

[1] http://sepem.eu/
[2] http://sepem.eu/help/data_sources.html
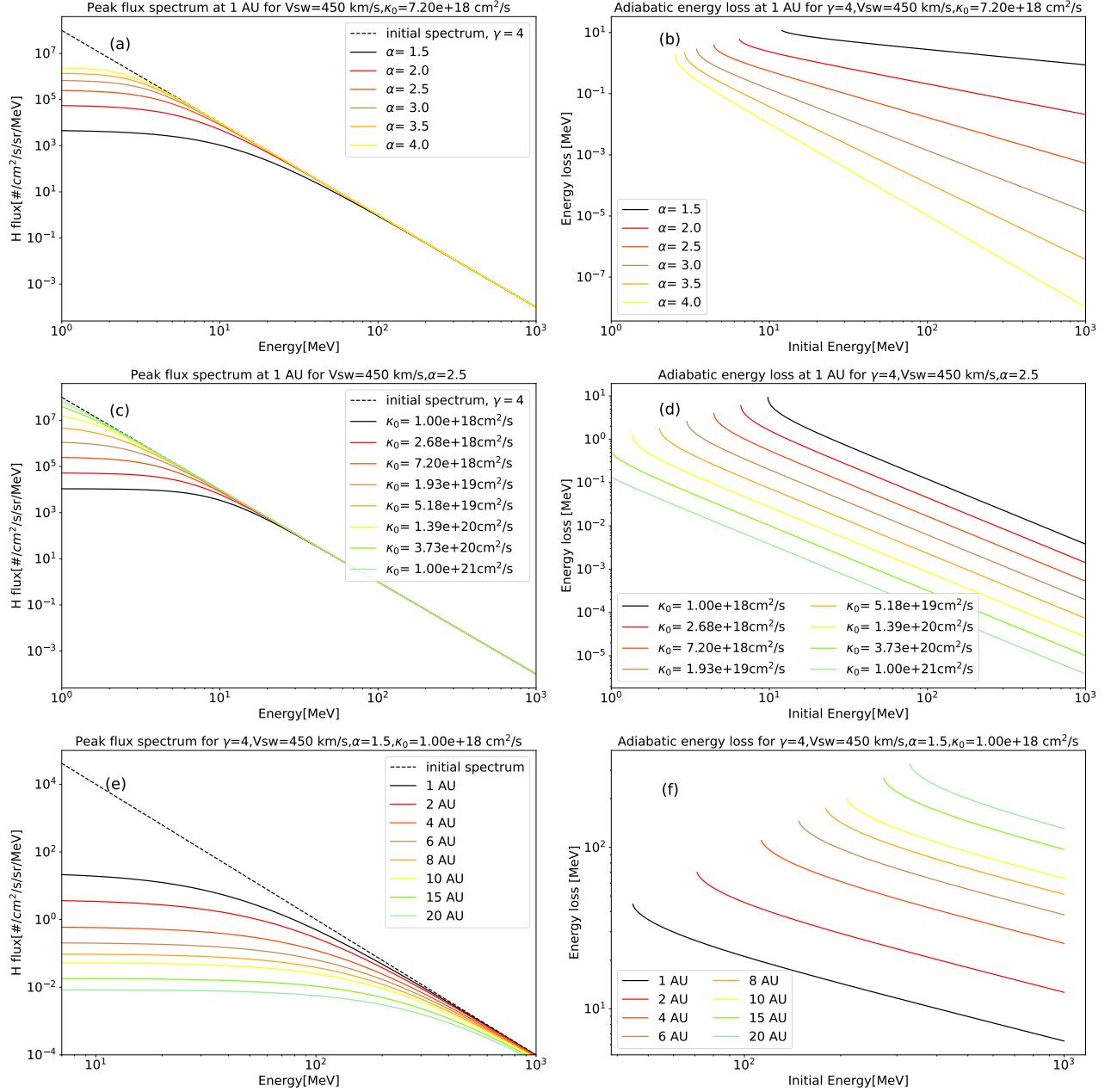
Figure 1. Impact of adiabatic energy loss on the particle energy spectrum as described by Eq. 9. We set an initial flux spectrum with parameters $j_0 = 10^8[\#/\mathrm{cm}^2/\mathrm{s}/\mathrm{sr}/\mathrm{MeV}]$, $\gamma = 4$, and a constant solar wind speed of V_{sw}=450 [km/s]. Panel a shows the peak flux spectrum at 1 AU for different diffusion coefficient index α. Panel b shows the adiabatic energy loss of particles with a given initial energy corresponding to Panel a. Panel c shows the peak flux spectrum at 1 AU for different diffusion normalization coefficient κ_0. Panel d shows the adiabatic energy loss of particles with a given initial energy corresponding to Panel c. Panel e shows the evolution of the peak flux spectrum at different heliocentric distance. Panel f shows the adiabatic energy loss corresponding to Panel e.

For each energy channel we use the geometric mean of upper and lower limit as the effective energy (see Table 1).

We note that the uncertainty in the flux values is not provided in the SEPEM dataset and it is nontrivial to derive it as the flux is rebinned into energy bins different from those used directly for measurements. Since the resulting uncertainties on the fit parameters do not affect our subsequent analysis and results, we assign an arbitrary uncertainty of 5% to all energy channels to complete the fitting algorithm following previous studies (e.g., Dierckxsens et al. 2015).

3.2. SEPEM reference event list

At present, there is no world-wide consistent definition of the start and end time for SEP events. The SEPEM project selected 7.23–10.46 MeV proton channel as the reference channel and generated a reference SEP event list[3] based on the following standards (Jiggens et al. 2011): (1) Threshold for the start and end of an event: 0.01 [#/cm^2/s/sr/MeV]. (2) Minimum peak flux: 0.5 [#/cm^2/s/sr/MeV]. (3) Minimum event duration and dwell time: 24 h.
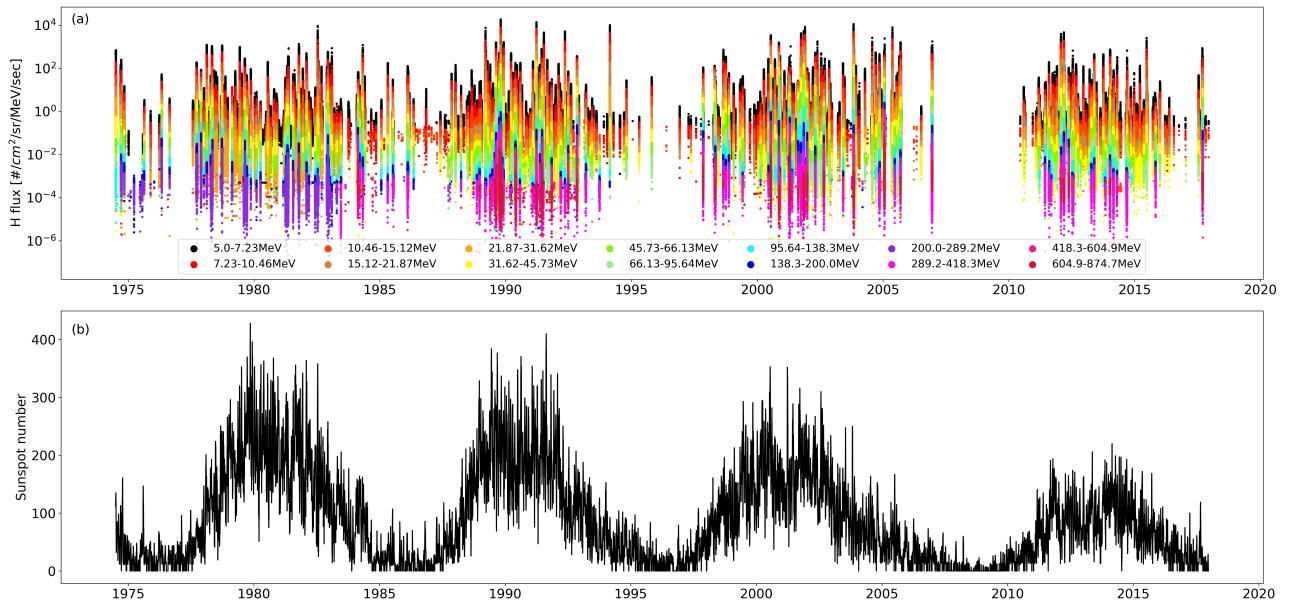
Figure 2. Occurrence of SEP events is related to the solar activity cycle. Panel a shows the entire SEPEM dataset used in this study, namely the SEP proton flux-time profile from July 1, 1974 to December 31, 2017. Each vertical colored strip represents an SEP event, with different colors indicating various energy bins. Panel b shows the corresponding daily Sunspot Number (SSN) for the same time duration. The frequency of SEP events is positively correlated with SSN indicating solar activities.

Fig. 2 shows the entire SEPEM dataset used in this study (panel a), along with the corresponding daily Sunspot Number (SSN) for the same time period (panel b). The SSN data are accessed from the World Data Center SILSO[4], Royal Observatory of Belgium, Brussels (SILSO World Data Center 2006–2022). As expected, more SEP events occur during periods of high solar activity. There are also quite a number of events occurring in the rising and decay phases of solar cycles. This is a

---

[3] http://sepem.eu/help/event_ref.html
[4] Solar Influences Data Analysis Center https://www.sidc.be/SILSO/datafiles

well-known feature of SEP events and poses great challenges to the prediction of the occurrence and intensity of SEP events.

By the definition of single SEP event in the original SEPEM reference event list, there may be more than one enhancements from several events (namely, the "single" event can be further divided into several events with individual rising, peak and declining phases). This could lead to an incorrect peak flux selection. So we modified the start and end times of the original SEPEM reference event list to make both the peak energy spectrum and integrated energy spectrum related to the same SEP event. More details can be found in Sect. 4, Table 3 and Table 4[5].

3.3. *Spectra Fitting Methods*

Considering the forms of Eqs. 3 and 9, we utilize the nonlinear least squares method to obtain the optimal fitting parameters by minimizing the sum of squares error function $S(\boldsymbol{\theta})$ with the following definition (Vugrin et al. 2007):

$$S(\boldsymbol{\theta}) = \sum_{i=1}^{n} \left[f\left(\boldsymbol{\theta}; \mathbf{x_i}\right) - y_i \right]^2 = \sum_{i=1}^{n} \left[r_i(\boldsymbol{\theta}) \right]^2,\tag{10}$$

where $f\left(\boldsymbol{\theta}; \mathbf{x_i}\right)$ is the nonlinear model, $\boldsymbol{\theta}$ is a vector of all parameters, and $r_i(\boldsymbol{\theta})$ is residual.

Figure 3 shows an example of spectrum fitting. Panel a shows the flux time profile of a SEP event during November 1997. The black circles represent the peak flux of each energy bin. Panel b shows the peak flux spectrum fitting. Panel c shows the integrated fluence spectrum fitting throughout the event.

We note that there are still tens of events whose spectra can be fitted by neither Eq. 3 nor Eq. 9. There are multiple reasons for this, such as significant impact of the previous SEP event, influence of magnetic field structures on the SEP flux evolution, or other obvious instrumental or systematic errors. These events are excluded from the table and the following study.

4. RESULTS AND DISCUSSIONS

Fitting parameters for the peak flux spectra following Eq. 9 are listed in Table 3. As mentioned in Sect. 3.1, the uncertainties are calculated assuming a 5% arbitrary dataset uncertainty. κ_0_450 is calculated using a constant solar wind speed of 450 [km/s], while κ_0 is calculated using the mean solar wind speed in the 6 days after the events onset. The corresponding solar wind speed values and standard deviations are listed in columns "Vsw" and "Vsw_err". The solar wind speed data is obtained from GSFC/SPDF OMNIWeb interface[6]. We also obtained corresponding X-ray flare class for each SEP event from NOAA space environment services center[7] for further analysis in Sect. 4.4.

Fitting parameters for the time-integrated fluence spectra, namely Eq. 3, are listed in Table 4 where $E_{break} = E_0\left(\gamma_1 - \gamma_2\right)$ is the transition energy of the Band function. The GLE event list is obtained from the Neutron Monitor GLE database[8].

The calculation of the chi-square value for energy spectrum fitting is as follows:

$$\chi^2 = \frac{1}{N} \sum_{k=1}^{N} \frac{\left[j_{\text{Fit}}\left(E_k\right) - j_{\text{Meas}}\left(E_k\right) \right]^2}{\sigma_k^2},\tag{11}$$
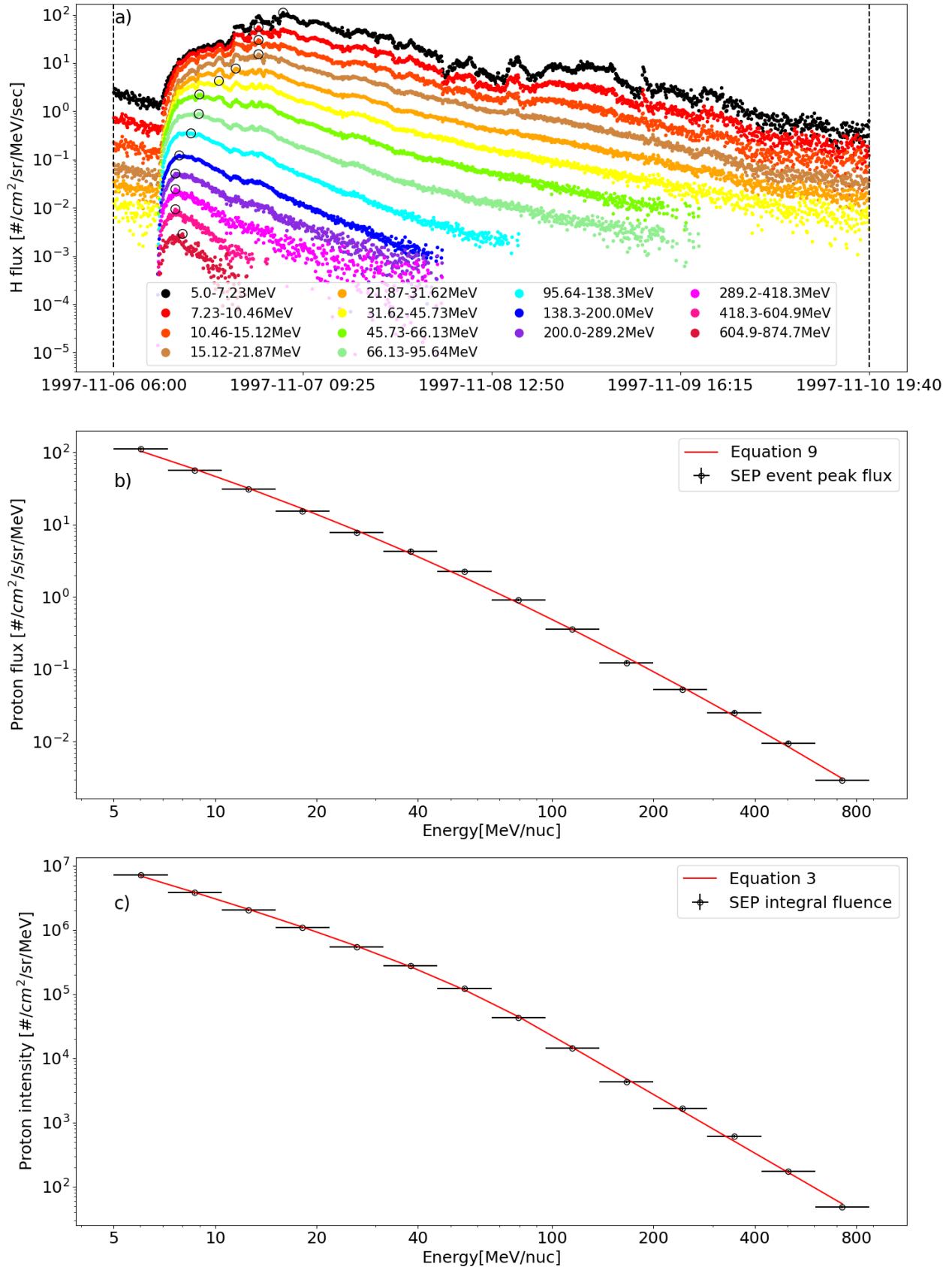
Figure 3. Example of spectrum fitting. Panel a shows the flux time profile of a SEP event during November 1997. The black circles represent the peak flux of each energy bin. The vertical dashed lines indicated the start and end time for the integrated fluence spectrum. Panel b and c show the peak flux spectrum and the integrated fluence spectrum fitting, respectively.
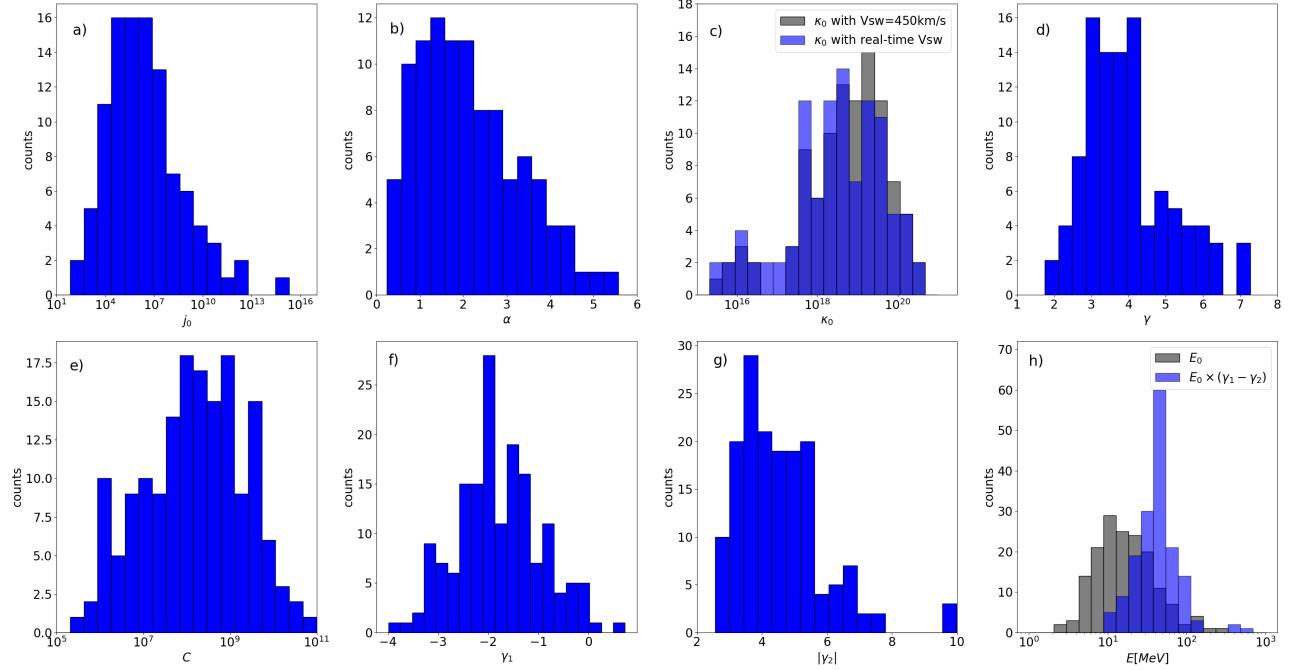
Figure 4. Histograms of the fitting parameters shown in Table 3 and Table 4. The results of the Anderson–Darling test are shown in Table 2, indicating that logC, γ_1, and logE_0 follow a normal distribution.

in which N is the number of energy bins, $j_{\mathrm{Fit}}(E_k)$ and $j_{\mathrm{Meas}}(E_k)$ are the fitted and measured particle flux at the kinetic energy of E_k, respectively. $\sigma_k = 0.05 j_{\mathrm{Meas}}(E_k)$ represents the aforementioned uncertainty on the data in the kth bin.

As we can see from Table 3 and Table 4, there are a significant number of events for which the value of χ^2 is relatively large. The reasons for large χ^2 value may be divided into two categories: One comes from the data processing algorithms. Data of SEP flux in the four highest energy channel of Table 1 can be significantly influenced by the GCR background subtract algorithms, which makes the fitting of this part difficult. The other reason is the influence of local acceleration and propagation effects which are not considered in the model used here.

4.1. *Distribution of spectral parameters*

We analyze the peak flux spectra of 103 events and the integral fluence spectra of 164 events in total. The other 160(99) events listed in the reference event table are not involved in the following analysis as mentioned in Sect. 3.3.

The histograms in Fig. 4 show the distribution of fitting parameters listed in Table 3 and Table 4. Panel c illustrates the distribution of $\kappa_{0\_}450$ obtained through the utilization of a constant solar wind speed of 450 [km/s], and κ_0 derived from real-time solar wind speed observations near Earth. Our subsequent analysis relies on the κ_0 derived from real-time solar wind speed. The histograms show that the utilization of a constant solar wind speed does not appear to have a significant impact on the distribution of this parameter, but it may differ significantly for individual events as shown in Table 3.

To better quantify their distribution feature, we further investigated the distribution of fitting parameters using the Anderson–Darling test (Anderson & Darling 1954) with the results shown in

Table 2. Anderson–Darling test (significance level equals to 0.05) for fitting parameters.

Parameter	statistic	critical value	Parameter	statistic	critical value
$\log j_0$	1.23	0.76	$\log C$	0.49	0.77
α	1.71	0.76	γ_1	0.41	0.77
$\log \kappa_0$	1.01	0.76	γ_2	4.94	0.77
γ	1.83	0.76	$\log E_0$	0.68	0.77

Table 2. It can be seen that the statistical values of parameters $\log C$, γ_1, and $\log E_0$ are less than the critical value for a significance level of 0.05. This indicates that they mostly follow a normal distribution. More discussions will be given in Sect. 5

4.2. *Relationships between integral fluence spectra and peak flux spectra*

We now try to find out whether the peak flux spectrum and integral fluence spectrum of the same SEP event have a certain kind of correlation. Fig. 5 demonstrates the relationships among 8 fitting parameters. For each SEP event indicated by a dot or circle, the four parameters of the peak flux spectrum (Eq. 9) are plotted on the x-axes, while the four parameters of the integral fluence spectrum (Eq. 3) are plotted on the y-axes. Solid dots are fitted parameters of GLE events, while parameters of other SEP events are represented by hollow circles. The red line represents the linear regression curve of two parameters for both GLE events and non-GLE events, and the corresponding linear regression function is shown in the legend. The shaded area represents the confidence interval for one standard deviation. From the graph, we can summarize some interesting relationships between the two sets of parameters:

1. In panel a, the two normalization coefficients, C and j_0, have a clear positive correlation. This is reasonable: if more SEPs are released at the source region, it is expected that a greater number of SEPs will be detected at Earth. Once SEPs are released from the acceleration source, they will propagate in different directions. However, we only have data for the Earth's orbit from the SEPEM dataset, which could result in the dispersion of this positive correlation.

2. In panel d, the normalization coefficients C and SEPs' source spectrum index γ also have a positive correlation indicating that events with larger fluence at lower energy range more likely result from a softer SEP spectrum. There may be two reasons for this. One reason is that the SEPEM reference event list has a strict definition of SEP events (see Sect. 3.2) with the original intention to exclude particle enhancement events of non-solar origin from the list, such as those accelerated by Stream Interaction Regions. This, however, has resulted in some weaker SEP events also being excluded from the list. These events have a smaller normalization coefficients C and a larger spectrum index $|\gamma|$ so that they do not have enough particles within the energy range of 7.23-10.46 MeV to define an SEP event in the SEPEM list. This can explain why there is no distribution of data points in the lower right part of this panel.

3. Panel d also shows that there lack events with both very large intensities and small γ values. An early study by Fichtel & McDonald (1967) estimated that the total energy of particles in a
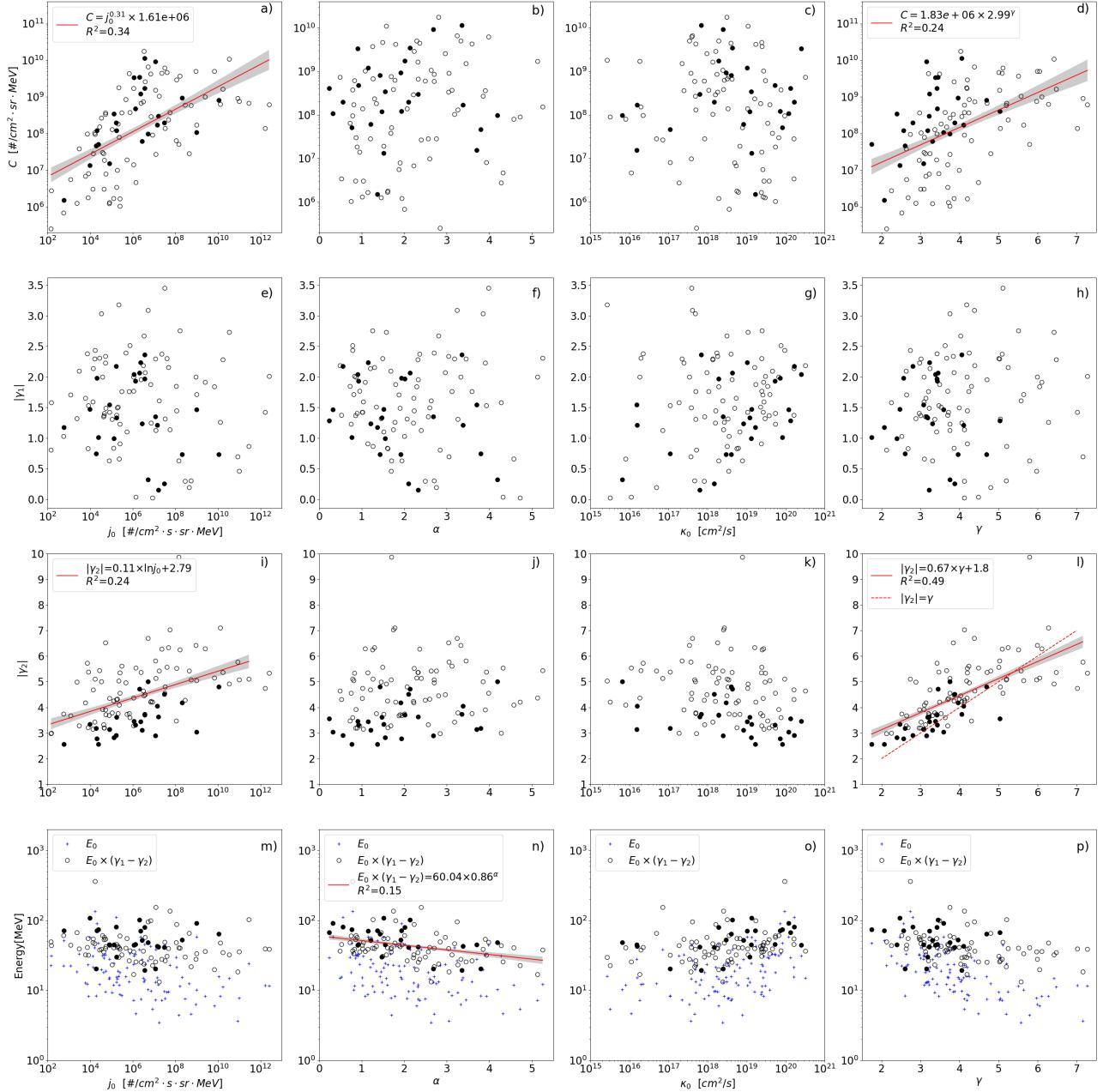
Figure 5. Relationships among 8 fitting parameters. For each event, the four parameters of the peak flux spectrum (Eq. 9) are plotted on the x-axes, while the four parameters of the integral fluence spectrum (Eq. 3) are plotted on the y-axes. Solid dots are parameters of GLE events, while parameters of other SEP events are represented by hollow circles. In each panel where the R^2 is larger than 0.1, the red line represents the linear regression curve between two parameters for all events, and the corresponding linear regression function is shown in the legend. The shaded area represents the confidence interval for one standard deviation. The red dashed line in panel l represents the function of $|\gamma_2| = \gamma$.

large SEP event was about 10^{30}[ergs], roughly 1 percent of total energy of a flare. Emslie et al. (2012) evaluated the energy budget of 38 large solar eruptive events between 2002 and 2006, and found that the SEP energy was between $\sim 0.1\%$ and 3.5% of the total eruptive energy.

For instance, they estimated that SEPs in GLE event Nr. 65 carried the highest energy of 4.3×10^{31}[ergs], which was about 1.5% of the estimated free magnetic energy ($\sim 3 \times 10^{33}$[ergs]) of the X17 flare. The SEP spectrum is constrained by the total energy of accelerated particles: $\int EjdE = \frac{j_0}{\gamma-2}(E_{min}^{2-\gamma} - E_{max}^{2-\gamma})$. For a given energy limit, the larger the intensity scaling factor j_0 (flux at 1 MeV), the steeper the spectrum (with a larger $|\gamma|$).

4. In panel l, we can observe a strong positive correlation between the spectral indices of the high-energy portion of the integral spectra $|\gamma_2|$ and the initial spectra γ and we fit them as $|\gamma_2| = 0.67 \times \gamma + 1.8$. The results of linear regression is not far from the function of $|\gamma_2| = \gamma$, which is represented by the red dashed line. This reason that $|\gamma_2|$ differs from γ for single events may be a result of the combined effects of adiabatic energy loss and multiple crossing effects related to particle scattering (Chollet et al. 2010). The former tends to result in a softer spectrum ($|\gamma_2| > \gamma$) as higher-energy particles lose their energy to become lower-energy ones, while the latter modifies a spectrum to become harder ($|\gamma_2| < \gamma$) as high-energy particles are more likely to be observed multiple times at a given location.

5. Alternatively, the correlation between γ and γ_1 as shown in panel h is less obvious. This is because lower energy particles experience more transport effects given their smaller mean free path length (Lario et al. 2007). These effects include the aforementioned adiabatic energy loss and multiple crossing as well as cross-field diffusion and pitch angle scattering.

6. Combining panel l and panel i, it can be observed that when there is an enhancement of particle acceleration in the SEP source region (namely, larger j_0), the SEP source spectrum tends to become softer (namely, larger γ and $|\gamma_2|$). This suggests that there might be some energy constraints in the process of SEP acceleration as mentioned in Item 3, or that enhanced acceleration tends to prioritize the energization of low-energy particles as it takes longer time to accelerate particles to higher energies according to the diffusive shock acceleration mechanism (Decker & Vlahos 1986).

7. Four panels at the bottom show the relationship between peak spectral parameters and the transition energy of the Band function: $E_{break} = (\gamma_1 - \gamma_2) E_0$. A larger diffusion coefficient power-law index α or a larger SEP event source energy spectrum index γ tends to result in a smaller transition energy. This indicates that the transition energy may be a result of the propagation process. Considering adiabatic cooling process which depends on κ and α, we have shown that the peak energy flux of the low-energy region is more significantly reduced with smaller α, as unveiled in panel a of Fig. 1, which results in a larger transition energy in the Band function.

8. GLE events are registered when sufficient number of high-energy particles can overcome Earth's magnetic shielding and generate secondary particles in Earth's atmosphere to trigger ground neutron detectors. Thus, by definition, GLE spectra contain an enhanced high-energy component. This is shown in our plots: As marked by solid dots in each panel, GLE events typically have larger overall fluence normalization coefficients, C, harder SEP source spectra (smaller γ), as well as harder integral fluence spectra of the high-energy part (smaller $|\gamma_2|$) and higher transition energies of the Band function.
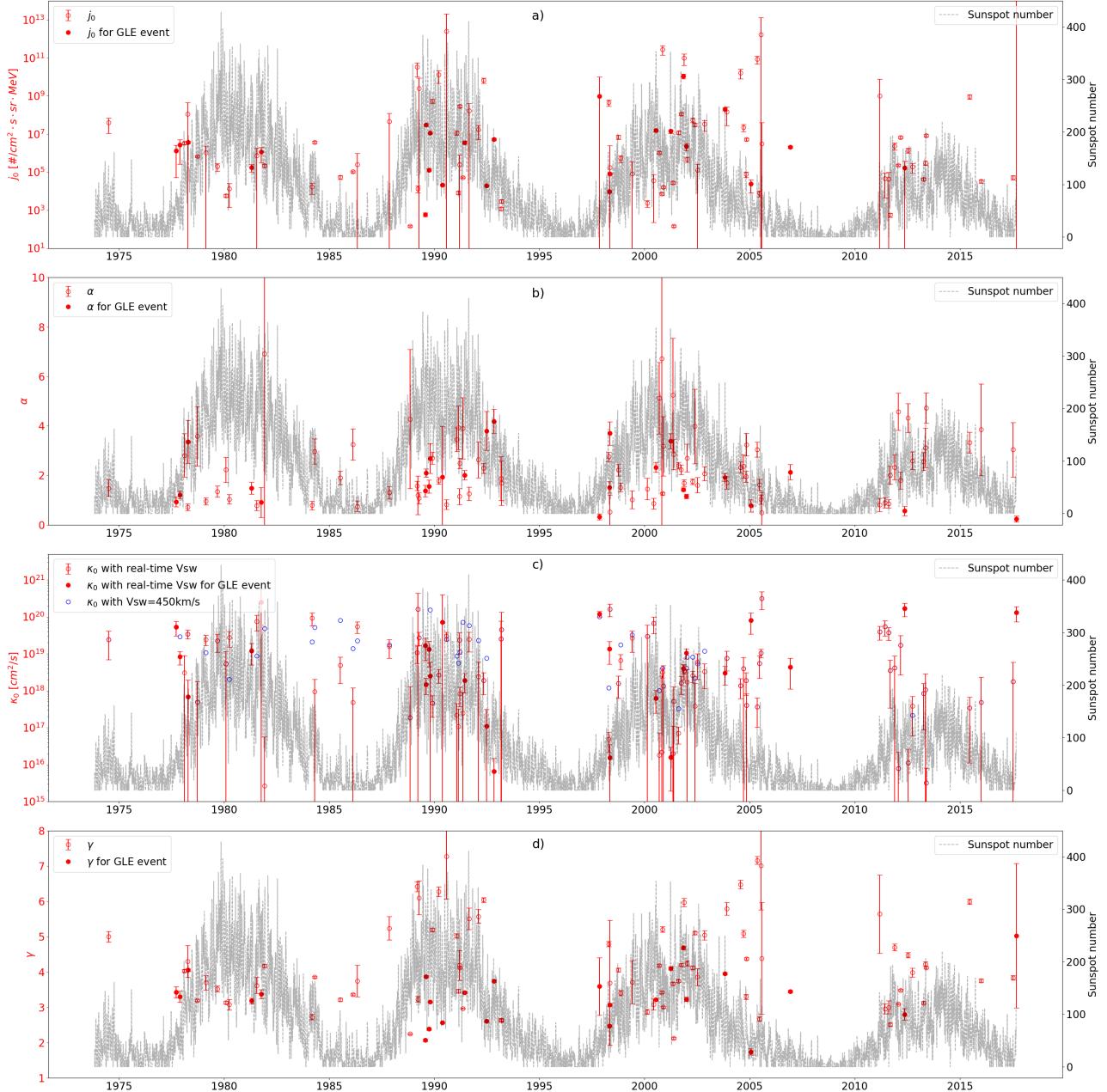
Figure 6. Solar-cycle evolution of four parameters in the peak flux spectrum as shown by the left y-axes, namely, j_0, α, κ_0, γ in Eq. 9 for a, b, c, d panels respectively. The uncertainty of each parameter results from assuming a 5% uncertainty in the SEPEM dataset as mentioned in Sect. 3.1. Solid dots are parameters of GLE events. The black lines in the background represent the daily sunspot number as scaled by the right y-axes.

4.3. *Spectral evolution over the solar cycle*

It has been almost 200 years since the discovery of the ~11-year solar activity cycle(e.g., Hathaway 2015). As shown in Fig. 2, the occurrence of SEP events is closely related to the solar activity cycle. Due to the extensive coverage of the SEP event list studied in this work, which spans almost four
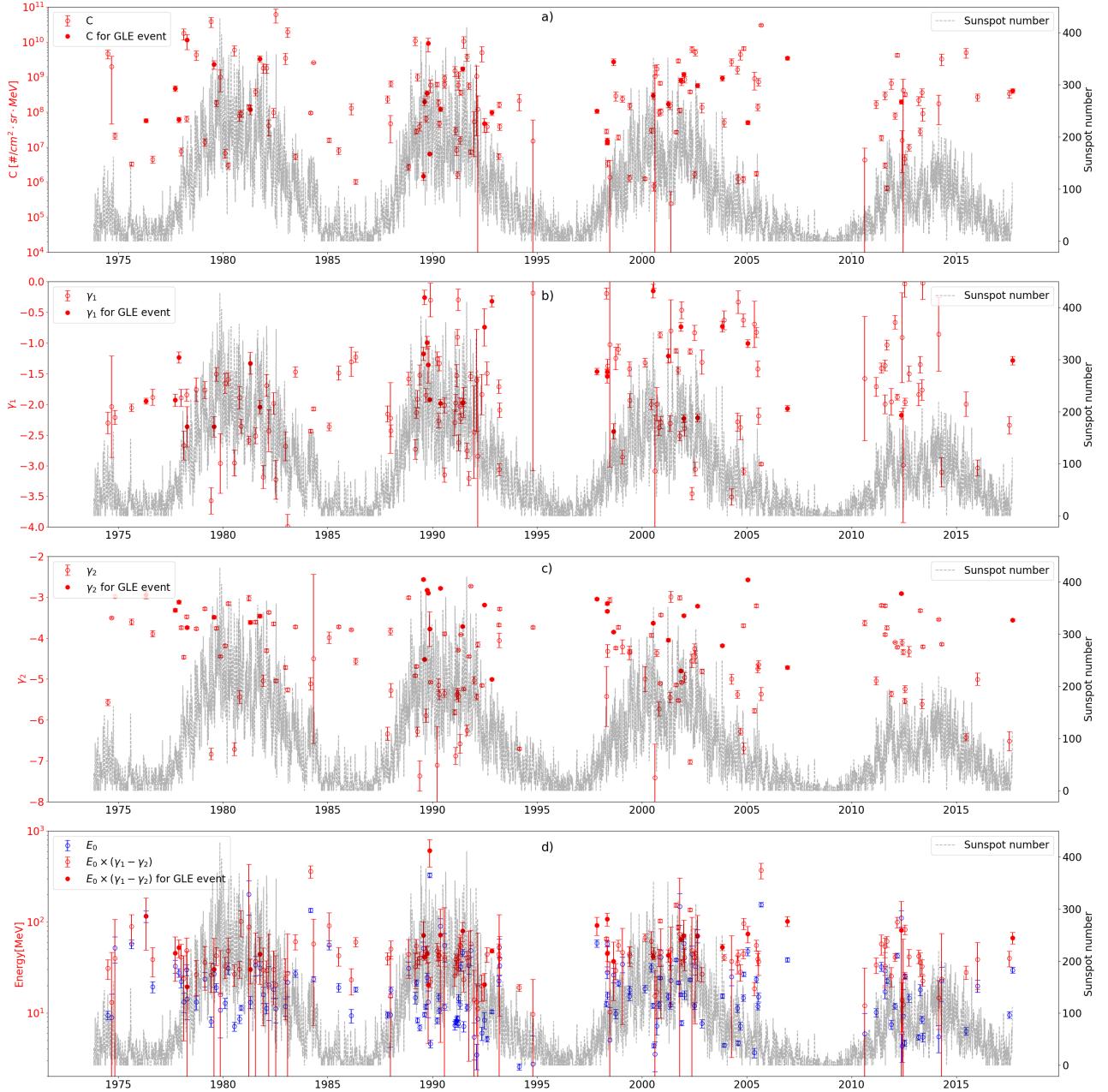
Figure 7. Solar-cycle evolution of four parameters in the integral fluence spectrum in Eq. 3 as shown by the left y-axes. The uncertainty of each parameter results from assuming a 5% uncertainty in the SEPEM dataset as mentioned in Sect. 3.1. Solid dots are parameters of GLE events. The black lines in the background represent the daily sunspot number as scaled by the right y-axes.

solar cycles, it is possible to conduct statistical research on the energy spectra of SEP events during various solar activity phases.

Figure 6 demonstrates the time distribution of four parameters in the peak flux spectrum (Eq. 9). Figure 7 demonstrates the time distribution of four parameters in the integral fluence spectrum (Eq. 3). Solid dots are parameters of GLE events. The black lines in the background represent the daily sunspot number.
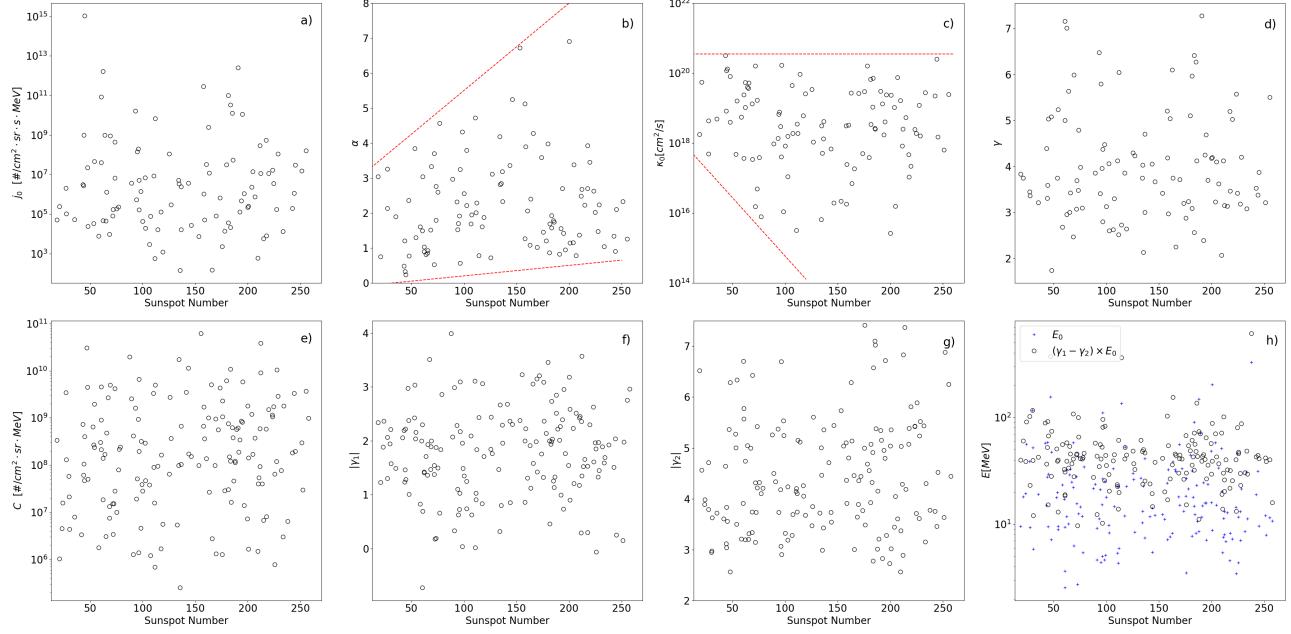
Figure 8. Distribution of the energy spectrum parameters versus the sunspot number. We use the monthly-averaged SSN centered at each SEP event's start time. The red dashed lines illustrate the distribution boundaries of α and κ_0 with respect to sunspot number.

In Fig. 8, we examine the relationship between the energy spectral parameters and the sunspot number. Since the sunspot number is only a proxy for the solar activity and its daily values are highly fluctuating, we use the monthly-averaged SSN centered at each SEP event's start time, and we do not label the GLE event separately. The red dashed lines illustrate the distribution boundaries of α and κ_0 with respect to sunspot number.

In Fig. 9, we further examine the diffusion coefficient evolution over the solar cycle. Panel a shows the results of the diffusion coefficient $\kappa = \kappa_0 E^\alpha$ calculated for protons of 1, 10, 100, and 300 MeV. We consider monthly-averaged SSN less than 70 as low solar activity periods and those greater than 200 as high solar activity periods. The distributions of κ of protons with different energies for the above two solar activities are compared in panels b, c, d and e.

We can see from Figures 6-9 that:

1. The diffusion effect of SEPs is solar-cycle dependent. In Fig. 6(b),(c) and Fig. 8(b),(c), we can observe a weak solar cycle evolution of the fitted parameters κ_0 and α which define the diffusion coefficient κ. In Fig. 9, we can better see that during higher solar activity periods, both α and κ_0 show a wider distribution: α can reach a larger magnitude than during solar maximum periods, while κ_0 can reach smaller values compared to solar quiet periods. This suggests that the difference in the diffusion behavior of SEPs with different energies is larger during solar maximum periods.

2. Fig. 9 further illustrates the cycle-dependent diffusion coefficient of different energies (1, 10, 100 and 300 MeV protons in panels b,c,d,e, respectively). Both distribution and median value of diffusion coefficient indicate that low-energy particles (1 MeV, panel b) experience enhanced diffusion (smaller κ) during higher solar activities; high-energy particles (100 and 300 MeV,
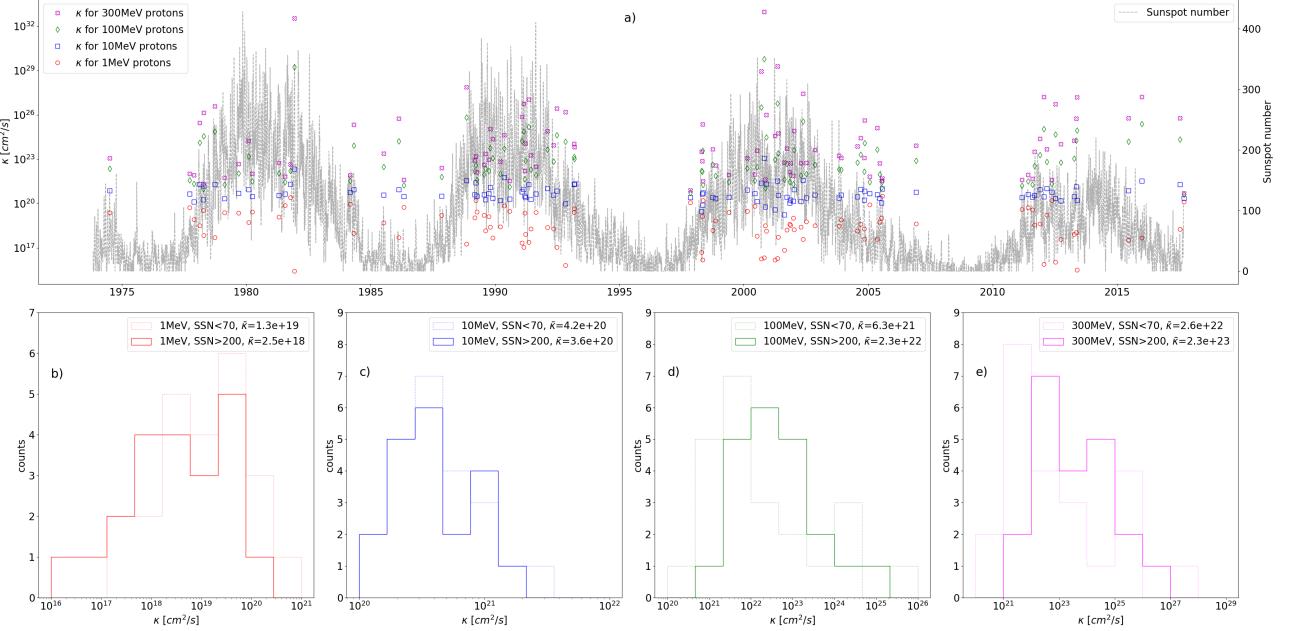
Figure 9. Solar-cycle dependent diffusion coefficient of different energies. Panel a shows the solar cycle evolution of the diffusion coefficient (left y-axis), which is defined by Eq. 6, for four different energies of protons (left legends). The gray lines in the background represent the daily sunspot number as scaled by the right y-axis. Panels b, c, d, and e show the diffusion coefficient distribution of 10, 50, 100, and 300 MeV protons respectively. The distributions for low solar activity are represented by the dashed line, and for high solar activity are represented by the solid line. The median value of the diffusion coefficient $\bar{\kappa}$ for each distribution is also displayed in the legends.

panels d and e), however, experience reduced diffusion during higher solar activities. This result agrees with the modeled results of the propagation of cosmic rays, see Fig. 10 of Fiandrini et al. (2021) and Fig.4 of Song et al. (2021). The quasi-linear theory (QLT) predicts that the two parameters α and κ_0 are related to the power spectrum of the interplanetary magnetic field (IMF) turbulence. The power spectral index of the IMF turbulent level varies with different levels of solar activity, leading to changes in the scattering behavior of charged particles with different energies (Fiandrini et al. 2021).

3. Other parameters, including j_0, γ, C, γ_1, γ_2 and the break energy, do not show significant changes with varying sunspot numbers. This suggests that despite of the reduced occurring frequency, the SEP events during solar minimum are not necessarily weaker than those during solar maximum. So it is equally important to predict SEP events throughout different solar activity cycles.

4.4. *Relationship with X-ray flare class*

At last, we examine the relationship between the energy spectrum parameters of the SEP event and the peak X-ray flux[9] of the corresponding flare. As shown in Fig. 10, the following conclusions can be drawn:

---

[9] Obtained from https://www.swpc.noaa.gov/
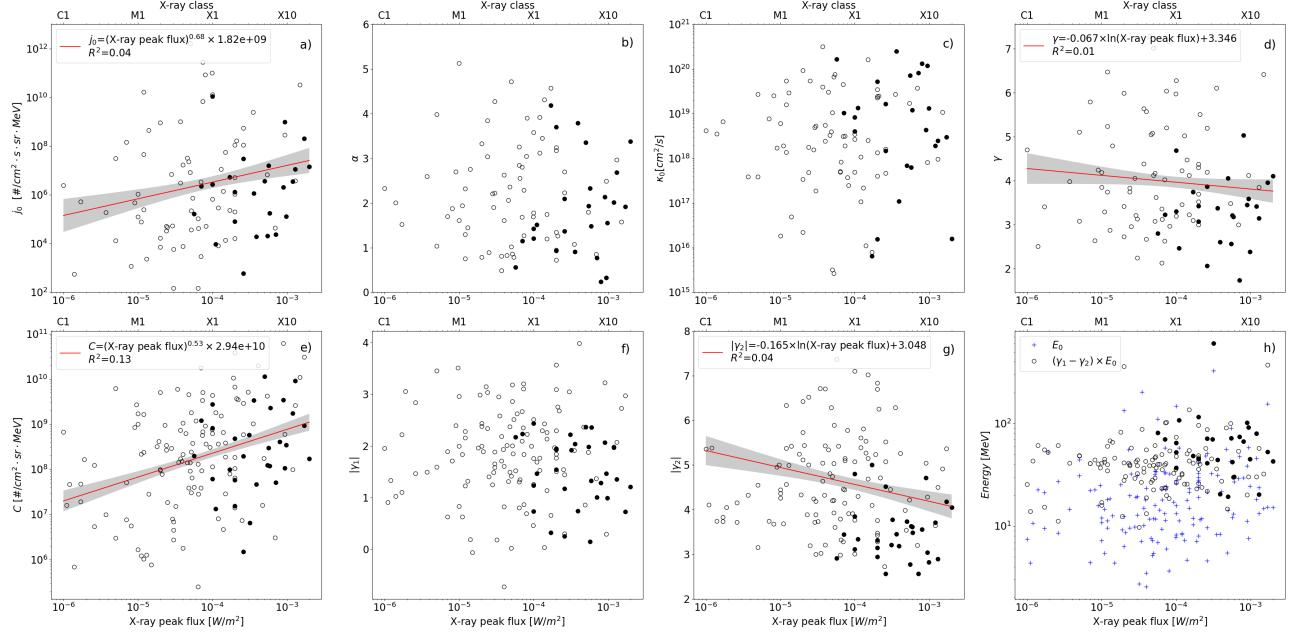
Figure 10. Relationship between the energy spectrum parameters of the SEP event and the peak X-ray flux of the corresponding flare. Solid dots are parameters of GLE events, while parameters of other SEP events are represented by hollow circles. The red line represents the linear regression curve, and the corresponding linear regression equation is shown in the legend. The shaded area represents the confidence interval for one standard deviation.

1. There is a positive correlation between the normalization coefficient of energy spectrum and the peak X-ray flux (see Fig 10 (a) and (e)). This means that larger solar flares are usually accompanied by a greater flux of SEPs. This resuls agrees with previous studies (Belov et al. 2007; Kahler et al. 2007).

2. The initial energy spectrum of SEPs, indicated by γ, and the spectrum of high-energy SEPs, indicated by γ_2, are generally harder (see Fig 10 (d) and (h)) for larger solar flares. This suggests that stronger solar flares can produce more high-energy SEPs.

3. The black solid dots representing the GLE event are distributed on the right side of all panels. This is an obvious result as these events usually correspond to solar flares of higher levels.

4. As the peak X-ray flux increases, the other four parameters, α, κ_0, γ_1, and $E_0(\gamma_1 - \gamma_2)$ do not show a significant trend of change (see Fig 10 (b), (c), (f), and (h)). This may be because these four parameters are mainly related to the propagation effect of SEPs in space. Even though a strong solar flare event and associated CME could sometimes alter the characteristics of solar wind plasma in interplanetary space, these changes are typically the outcome of the propagating SEPs and can be observed only later after the SEP event (Gopalswamy et al. 2004).

5. SUMMARY AND DISCUSSION

Considering the effects of diffusion-dependent adiabatic cooling on SEPs propagation, we propose a modified power-law function (Eq. 9) for the peak flux spectrum of SEP events. For the event-

integrated spectrum, we utilize the widely-accepted Band function (Eq. 3) to extract information about particle distribution. Further employing the continuous and high-quality SEPEM dataset, we are able to study SEP events covering a period of 43 years for about 4 solar cycles from 1974 to 2018. We further study the peak spectrum and event-integrated spectrum for each event and fit them with the aforementioned functions to derive the fitting parameters which indicate the physical properties as well as the acceleration and transport mechanisms of SEPs.

We found that the propagation of SEPs in the inner solar system is slightly modulated by the level of solar activity, which is similar to the previous numerical research results on the propagation of cosmic rays (see Sect. 4.3). This helps us gain a better understanding of the propagation mechanism of charged particles in the interplanetary magnetic field.

In order to further investigate the acceleration mechanism of SEPs, we examine the relationship between the energy spectrum parameters of the SEP event and the peak X-ray flux of the corresponding flare. As shown in Sect. 4.4, we found that larger SEP events, such as GLE events characterized by higher particle flux j_0 and harder energy spectra (smaller γ), correspond to flares of a higher-level. The power-law relationship in Fig. 10 panel a, is similar to that in other studies (e.g., Belov et al. 2007; Kahler et al. 2007) which, however, used either the peak proton flux of a specific energy range or the integrated X-ray flux. This can be explained by Big Flare syndrome mechanism: The statistically expected magnitude of measured flare energy manifestation is proportional to the energy released in a solar flare (Kahler 1982).

The reason for the double power-law characteristics of the SEP spectrum has not been clearly understood to this day. The understanding of transition energy or break energy is crucial for this topic. Based on correlation between break energy and charge-to-mass ratio, several numerical simulation studies suggest that the double power-law spectrum of SEP events can be directly generated by the acceleration at the shock (e.g., Mason et al. 2012; Desai et al. 2016; Yu et al. 2022). Alternatively, Mason et al. (2012) set the initial energy spectrum as a double power-law and found that as particles propagate, the transition energy of the spectrum decreases. Other numerical studies even suggest that the double power-law spectrum can be naturally built from an initial single power-law spectrum through particle propagation processes(e.g., Li & Lee 2015; Zhao et al. 2016).

By linking the peak flux spectrum which is closely related to the accelerated particle spectrum with the integral spectrum which contains more propagation effect, we can gain a better understanding of the acceleration and propagation behavior of particles. Based on the statistical analysis of 103 fitted SEP peak spectra and 164 fluence spectra, our study investigates the correlation between the transition energy of the double power-law spectrum and the particle diffusion coefficient (see Sect. 4.2). We note that the transition energy of the fitted Band function has a slight dependence on the diffusion coefficient, indicating that SEP propagation process can contribute to the formation and/or evolution of the double power law.

Moreover, as shown in Sect. 4.1, the three parameters in the Band function, $\log C$, γ_1, and $\log E_0$ approximately follow a normal distribution. We do not consider this to be a coincidence, but rather an indication that the physical processes determining these three parameters are different from the other parameters such as α, κ_0, and γ. Generally speaking, the time-integral energy spectrum can be considered as the superposition of a series of instantaneous energy spectra. During a single SEP event, the solar wind parameters in space can be approximated as constant, allowing the parameters of this series of instantaneous energy spectra to be considered to follow the same distribution. According

to the central limit theorem, the superposition of these parameters with the same distribution will follow a normal distribution.

Overall, we outline the mechanism for establishing the double power-law spectrum of particle propagation process as follows: During the descending phase of the SEP event, particles collected by the detector may have traveled a much longer distance (including the multiple-crossing process) than the particles which arrived during the early phase due to the spatial propagation effect (Wang & Qin 2023). Thus, during the descending phase transport effects including adiabatic cooling could significantly impact the spectra of SEPs as shown by simulations (Qin et al. 2006; Mason et al. 2012). Since low-energy particles experience greater relative energy loss compared to high-energy particles, there would be more flattening of the energy spectrum in the low-energy region, resulting in a double power law.

Further analysis and attribution of SEP properties due to either flare- and CME-acceleration mechanisms would help us better understand the acceleration nature and constrain of SEPs. Utilizing data collected at various solar distances rather than 1 AU would contribute to a better understanding of the transport effects and the spatial evolution. In order to fully understand SEP events, we require more comprehensive observation instruments that encompass a wider range of space, time, and energy.

Table 3. Peak flux spectral parameters fitted for 103 events.

No.	No.[1]	Start Time	End Time	j_0[2]	j_0_err[2]	α	α_err	κ_0-450[3]	κ_0[4]	κ_0_err[4]	γ	γ_err	V_{sw}[5]	V_{sw}_err[5]	χ^2
1	2	1974-07-03 01:00	1974-07-10 13:30	4.02E+07	2.91E+07	1.49	0.33	2.41E+19	2.41E+19	1.72E+19	5	0.15	571.96	122.74	24.6
2	9	1977-09-18 16:30	1977-09-23 07:30	1.32E+06	1.27E+06	0.93	0.2	5.26E+19	5.26E+19	2.22E+19	3.43	0.16	407.1	40.59	3.81
3	11	1977-11-22 11:00	1977-11-28 13:30	2.72E+06	2.46E+06	1.21	0.15	2.87E+19	8.24E+18	3.28E+18	3.31	0.16	351.04	65.76	6.15
4	14	1978-02-13 08:00	1978-02-22 21:30	3.40E+06	5.38E+05	2.81	0.87	3.24E+10	3.10E+18	5.80E+18	4.03	0.04	412.58	77.81	20.6
5	15	1978-04-08 04:00	1978-04-16 03:00	1.10E+08	3.49E+08	0.72	0.14	3.45E+19	3.45E+19	9.17E+18	4.3	0.45	491.45	76.29	16.31
6	16	1978-04-17 03:30	1978-05-05 02:30	3.69E+06	5.96E+05	3.36	0.87	6.84E+17	6.84E+17	1.27E+18	4.05	0.04	514.36	109.31	33.4
7	21	1978-09-23 11:30	1978-10-16 01:30	6.73E+05	7.60E+04	3.58	1.2	4.96E+17	4.96E+17	1.27E+18	3.2	0.03	544.32	150.63	3.46
8	24	1979-02-17 16:30	1979-02-23 08:00	1.07E+06	1.33E+06	0.95	0.14	1.08E+19	2.43E+19	7.47E+18	3.7	0.2	509.62	66.95	11.23
9	30	1979-09-08 12:00	1979-10-03 04:30	1.99E+05	8.68E+04	1.34	0.23	2.26E+19	2.26E+19	1.17E+19	3.52	0.08	322.92	16.64	6.87
10	34	1980-02-05 18:30	1980-02-09 18:30	5.83E+03	1.10E+03	2.23	0.51	5.36E+18	5.36E+18	6.11E+18	3.13	0.04	426.83	51.93	6.41
11	35	1980-03-29 19:30	1980-04-08 20:00	1.35E+04	1.21E+04	1.04	0.19	2.03E+18	2.75E+19	1.22E+19	3.08	0.15	400.85	66.06	5.77
12	42	1981-04-24 04:00	1981-04-26 11:00	1.75E+05	7.31E+04	1.48	0.24	1.20E+19	1.20E+19	7.04E+18	3.18	0.08	477.98	66.89	18.84
13	43	1981-07-20 15:00	1981-07-28 07:00	7.40E+05	1.07E+06	0.78	0.2	8.76E+18	7.58E+18	3.42E+19	3.62	0.22	494.18	124.13	11.15
14	48	1981-10-08 03:30	1981-10-26 22:30	1.14E+06	8.33E+05	0.91	0.61	2.51E+20	2.51E+20	3.10E+20	3.38	0.12	439.16	71.41	5.88
15	51	1981-12-05 17:00	1981-12-14 08:00	2.23E+05	3.54E+05	6.91	10.46	4.85E+19	2.66E+19	5.39E+16	4.18	0.05	353.87	64.71	0.11
16	66	1984-03-07 01:00	1984-03-23 07:00	1.67E+04	9.78E+03	0.79	0.17	2.10E+19	9.27E+19	3.64E+19	2.73	0.08	525.95	44.12	1.93
17	67	1984-04-25 09:30	1984-05-15 19:30	3.78E+06	5.00E+05	2.97	0.51	5.13E+19	9.53E+19	1.08E+18	3.86	0.03	534	11.86	43.56
18	71	1985-07-09 02:30	1985-07-12 13:30	5.33E+04	1.25E+04	1.9	0.27	8.03E+19	4.90E+18	3.32E+18	3.21	0.05	471.66	57.1	9.26
19	73	1986-02-14 10:55	1986-02-19 07:40	1.06E+05	1.27E+04	3.26	0.63	1.38E+19	4.88E+19	6.90E+17	3.37	0.03	479.32	45.99	5.88
20	75	1986-05-04 12:20	1986-05-05 13:15	2.47E+05	7.16E+05	0.75	0.22	2.27E+19	5.45E+19	1.85E+19	3.75	0.45	416.78	21.79	1.35
21	76	1987-11-07 22:45	1987-11-10 13:15	4.65E+07	7.61E+07	1.3	0.25	1.75E+19	1.59E+19	8.25E+18	5.24	0.33	530.58	107.19	0.17
22	80	1988-11-08 15:45	1988-11-10 11:40	1.47E+02	1.28E+01	4.28	2.82	1.86E+17	1.86E+17	1.09E+18	2.25	0.02	416.87	55	7.21
23	83	1989-03-08 03:30	1989-03-14 19:50	3.32E+10	2.32E+10	1.57	0.19	1.08E+19	1.08E+19	5.34E+18	6.42	0.15	543.96	152.17	78.63
24	84	1989-03-23 20:15	1989-03-24 21:30	1.37E+04	5.54E+03	1.2	0.78	1.62E+20	1.62E+20	2.71E+20	3.23	0.07	533.33	83.85	20.8
25	85	1989-04-10 21:15	1989-04-18 01:45	2.50E+09	6.33E+09	1.08	0.23	2.72E+19	2.72E+19	1.07E+19	6.1	0.48	402.14	30.24	1.66

Table 3 *continued on next page*

Table 3 (*continued*)

No.	No.[1]	Start Time	End Time	j_0[2]	j_0_err[2]	α	α_err	κ_0_450[3]	κ_0[4]	κ_0_err[4]	γ	γ_err	Vsw[5]	Vsw_err[5]	χ^2
26	89	1989-07-25 09:05	1989-07-26 17:45	5.90E+02	1.26E+02	1.37	0.24	1.66E+19	1.66E+19	9.97E+18	2.07	0.04	432.62	36.96	5.74
27	90	1989-08-12 15:45	1989-08-14 15:45	3.02E+07	4.87E+06	2.1	0.16	1.48E+18	1.48E+18	6.96E+17	3.87	0.03	530.51	92.08	42.99
28	92	1989-09-29 11:55	1989-10-10 05:20	1.30E+05	2.30E+04	1.55	0.26	1.32E+19	1.32E+19	8.74E+18	2.39	0.03	394.27	25.07	8.29
29	93	1989-10-19 13:10	1989-11-09 16:50	1.15E+07	1.12E+06	2.68	0.6	1.55E+20	2.49E+18	3.44E+18	3.15	0.02	609.32	150.42	12.75
30	95	1989-11-27 06:25	1989-12-05 09:05	5.52E+08	1.37E+08	2.7	0.24	4.64E+17	4.64E+17	2.74E+17	5.2	0.05	554.5	85.57	90.49
31	96	1990-03-19 06:30	1990-03-22 01:40	1.31E+10	8.51E+09	1.78	0.14	2.67E+18	2.67E+18	1.08E+18	6.28	0.13	447.1	96.56	60.07
32	102	1990-05-17 21:30	1990-05-24 19:00	2.09E+04	2.36E+03	1.93	2.05	7.12E+19	7.13E+19	3.26E+20	2.57	0.02	418.11	62.97	4.31
33	106	1990-07-31 15:25	1990-08-06 12:05	2.52E+12	1.84E+13	0.83	0.2	2.47E+19	3.03E+19	7.69E+18	7.28	1.21	441	60.6	0.88
34	108	1991-01-27 14:45	1991-02-02 19:30	1.14E+07	2.79E+06	3.45	0.48	8.68E+18	2.19E+17	2.32E+17	5.02	0.06	376.37	33.78	3.28
35	110	1991-02-25 10:40	1991-02-27 01:55	8.17E+03	1.57E+03	3.92	0.89	5.58E+18	1.08E+17	2.07E+17	3.46	0.05	422.79	48.27	47.11
36	111	1991-03-12 18:50	1991-03-13 22:25	2.50E+05	5.50E+05	1.15	0.32	2.34E+19	2.34E+19	1.37E+19	4.19	0.43	363.9	27.61	0.34
37	113	1991-03-23 06:40	1991-03-31 14:30	2.87E+08	4.12E+07	2.49	0.21	1.13E+19	8.15E+17	4.39E+17	4.12	0.03	478.67	13.01	61.51
38	116	1991-05-10 15:05	1991-05-15 10:50	5.20E+04	4.11E+03	3.9	1.24	7.11E+19	2.47E+19	6.51E+17	2.97	0.02	364.81	13.16	10.25
39	118	1991-06-09 19:10	1991-06-15 01:30	3.57E+06	6.14E+05	2.01	0.19	1.91E+18	1.91E+18	1.02E+18	3.42	0.03	541.21	73.29	18.18
40	120	1991-08-25 21:10	1991-08-30 22:30	1.66E+08	2.48E+08	1.26	0.27	5.86E+19	2.48E+19	1.36E+19	5.51	0.31	435.36	79.36	2.27
41	127	1992-02-06 22:45	1992-02-10 00:30	1.71E+07	1.20E+07	2.63	0.73	2.32E+19	2.45E+18	3.60E+18	5.57	0.19	461.75	58.05	0.61
42	130	1992-05-09 06:15	1992-05-13 20:15	6.84E+09	2.09E+09	2.29	0.21	1.91E+18	1.91E+18	1.13E+18	6.04	0.07	429.13	150.13	54.45
43	131	1992-06-25 20:30	1992-07-01 23:25	1.91E+04	1.58E+03	3.79	0.79	7.56E+18	1.10E+17	1.98E+17	2.61	0.02	536.66	41.41	10.18
44	133	1992-10-30 18:45	1992-11-01 21:20	5.29E+06	7.49E+05	4.19	0.49	6.46E+15	6.46E+15	8.09E+15	3.75	0.03	404.82	28.12	50.09
45	134	1993-03-04 13:20	1993-03-05 22:30	1.20E+03	2.31E+02	1.87	0.89	2.55E+19	2.55E+19	5.05E+19	2.64	0.04	416.61	77.49	7.2
46	136	1993-03-12 18:50	1993-03-14 15:05	2.98E+03	5.88E+02	1.69	0.89	4.50E+19	4.50E+19	8.95E+19	2.63	0.04	520.48	40.97	3.5
47	140	1997-11-04 06:50	1997-11-10 19:40	9.73E+08	9.04E+09	0.33	0.12	1.01E+20	1.19E+20	1.94E+19	3.59	0.82	371.21	38.3	3.84
48	141	1998-04-20 12:55	1998-04-26 15:05	4.52E+08	1.68E+08	2.76	0.19	1.19E+18	4.88E+18	2.76E+16	4.79	0.08	406.23	52.66	24.61
49	143	1998-05-02 13:55	1998-05-03 04:10	9.54E+03	1.70E+03	1.51	0.23	1.34E+19	1.34E+19	8.12E+18	2.47	0.03	547.41	85.11	3.7
50	144	1998-05-06 08:25	1998-05-08 00:20	8.13E+04	1.10E+04	3.7	0.47	1.54E+16	1.54E+16	1.95E+16	3.07	0.03	497.11	48.28	5.73
51	145	1998-05-09 06:50	1998-05-11 04:10	1.73E+05	2.25E+05	0.52	0.69	1.62E+20	1.62E+20	6.19E+19	3.7	1.77	426.97	74.82	2.12
52	149	1998-09-30 14:25	1998-10-04 04:20	7.04E+06	1.83E+06	2.21	0.23	1.57E+18	1.57E+18	9.53E+17	4.06	0.05	474.22	88.81	23.68

Table 3 *continued on next page*

Table 3 (*continued*)

No.	No.[1]	Start Time	End Time	j_0[2]	j_0_err[2]	α	α_err	κ_0_450[3]	κ_0[4]	κ_0_err[4]	γ	γ_err	Vsw[5]	Vsw_err[5]	χ^2
53	152	1998-11-14 06:30	1998-11-17 15:55	5.28E+05	2.14E+05	1.52	0.17	1.76E+19	6.62E+18	2.93E+18	3.41	0.08	432.73	51.39	12.13
54	156	1999-05-27 12:15	1999-05-28 14:40	8.15E+04	2.70E+05	1.02	0.36	3.29E+19	2.62E+19	1.51E+19	3.72	0.61	388.59	35.9	0.2
55	158	2000-02-18 08:45	2000-02-19 11:55	2.33E+03	8.73E+02	1.45	0.43	2.94E+19	2.94E+19	2.95E+19	2.88	0.07	436.73	136.37	20.87
56	161	2000-06-10 04:00	2000-06-12 21:10	3.68E+04	3.66E+04	0.86	0.22	6.65E+19	6.65E+19	3.15E+19	3.09	0.16	540.76	84.83	11.98
57	163	2000-07-13 00:30	2000-07-23 19:20	1.57E+07	2.03E+06	2.33	0.2	6.29E+17	6.29E+17	3.81E+17	3.22	0.02	661.16	135.08	11.81
58	166	2000-09-12 14:50	2000-09-18 01:25	1.07E+06	1.38E+05	5.13	1.45	1.02E+18	1.82E+16	5.45E+16	4.19	0.03	478.27	154	2.53
59	168	2000-10-25 15:15	2000-10-27 19:10	7.27E+03	9.58E+02	6.72	58.72	2.19E+16	2.19E+16	2.48E+18	3.42	0.04	377.28	32.77	0.61
60	170	2000-11-08 23:45	2000-11-15 17:00	2.84E+11	1.43E+11	1.27	0.05	4.05E+18	3.14E+18	9.34E+17	5.21	0.08	605.41	151.47	5.03
61	171	2000-11-24 07:00	2000-11-25 20:10	1.63E+04	1.88E+03	3.18	1.2	1.34E+18	1.34E+18	3.44E+18	3.01	0.03	497.56	71.98	10.93
62	176	2001-04-02 11:20	2001-04-07 08:20	1.42E+07	3.18E+06	3.38	0.3	1.57E+16	1.57E+16	1.38E+16	4.1	0.05	548.41	96.53	19.49
63	178	2001-05-07 15:00	2001-05-09 19:10	2.73E+04	4.38E+03	5.25	2.29	1.96E+16	1.96E+16	9.11E+16	3.67	0.04	474.33	80.86	4.02
64	179	2001-05-20 08:45	2001-05-21 14:25	1.46E+02	2.16E+01	2.84	0.61	5.14E+17	5.14E+17	7.61E+17	2.13	0.03	417.18	87.24	10.12
65	182	2001-08-16 00:55	2001-08-26 04:40	1.21E+07	2.45E+06	2.4	0.14	3.28E+17	7.03E+16	3.44E+16	3.75	0.04	459.33	77.22	8.39
66	183	2001-09-24 12:00	2001-10-12 03:05	1.13E+08	1.96E+07	2.23	0.2	1.61E+18	1.61E+18	8.27E+17	4.2	0.03	508.35	76.6	20.16
67	185	2001-11-05 16:55	2001-11-12 20:05	1.11E+10	3.20E+09	1.43	0.07	4.01E+18	4.01E+18	1.16E+18	4.69	0.05	482.65	98.21	8.26
68	186	2001-11-17 19:55	2001-11-30 13:00	1.01E+11	6.11E+10	1.69	0.13	3.46E+18	3.46E+18	1.52E+18	5.97	0.12	460.88	141.35	71.59
69	188	2001-12-26 05:55	2002-01-09 07:00	2.29E+06	9.54E+05	1.15	0.09	4.08E+18	1.04E+18	3.11E+18	3.23	0.07	416.91	65.95	7.92
70	189	2002-01-10 09:55	2002-01-18 18:35	4.76E+05	1.44E+05	2.7	0.56	8.15E+18	1.72E+18	2.10E+18	4.25	0.08	486.11	86.35	1.1
71	191	2002-04-17 11:30	2002-04-28 13:35	5.53E+07	1.48E+07	1.75	0.12	8.16E+18	2.53E+18	8.57E+17	4.12	0.05	492.63	56.64	29.08
72	192	2002-05-22 07:50	2002-05-25 00:15	3.10E+07	5.56E+06	3.98	1.5	2.15E+18	3.86E+17	1.18E+18	5.1	0.05	555.97	135.26	1.35
73	193	2002-07-07 14:00	2002-07-09 13:55	1.26E+05	1.41E+05	1.61	0.31	5.35E+18	6.03E+18	3.99E+18	3.86	0.24	431.76	44.02	1.08
74	200	2002-11-09 17:10	2002-11-11 21:15	3.29E+07	1.84E+07	2.06	0.29	1.17E+19	3.27E+18	2.13E+18	5.05	0.13	487.19	81.09	1.37
75	205	2003-10-28 03:30	2003-10-29 16:50	2.04E+08	3.53E+07	1.92	0.16	2.99E+18	2.99E+18	1.55E+18	3.96	0.03	663.49	204.97	21.88
76	207	2003-12-02 12:50	2003-12-06 06:05	1.46E+08	1.18E+08	1.7	0.24	7.66E+18	7.66E+18	4.24E+18	5.79	0.18	446.6	89.46	2.07
77	209	2004-07-23 15:05	2004-07-28 18:10	1.68E+10	8.63E+09	2.32	0.22	1.36E+18	1.36E+18	7.55E+17	6.48	0.12	623.09	141.75	4.77
78	211	2004-09-13 19:55	2004-09-17 18:15	2.28E+07	9.11E+06	2.36	0.47	3.97E+18	3.97E+18	4.03E+18	5.08	0.1	484.2	71.98	7.68
79	213	2004-11-01 06:10	2004-11-02 20:15	7.68E+04	2.56E+04	1.94	0.22	1.91E+18	1.91E+18	1.16E+18	3.3	0.07	399.63	86.18	14.57

Table 3 *continued on next page*

WANG & GUO

Table 3 (*continued*)

No.	No.[1]	Start Time	End Time	j_0[2]	j_0_err[2]	α	α_err	κ_0_450[3]	κ_0[4]	κ_0_err[4]	γ	γ_err	Vsw[5]	Vsw_err[5]	χ^2
80	214	2004-11-07 02:50	2004-11-09 02:45	5.25E+06	7.98E+05	3.24	0.46	4.03E+17	4.03E+17	4.25E+17	4.37	0.03	597.56	106.37	29.61
81	216	2005-01-20 01:00	2005-01-21 00:00	2.40E+04	1.57E+04	0.77	0.24	8.12E+19	8.12E+19	4.73E+19	1.74	0.09	694.59	152.67	9.11
82	218	2005-05-13 21:00	2005-05-17 12:30	8.58E+10	3.64E+10	3.04	0.3	3.69E+17	3.69E+17	2.66E+17	7.16	0.11	559.26	137.71	17.48
83	219	2005-06-16 20:50	2005-06-18 05:55	7.78E+03	2.65E+03	1.61	0.23	5.53E+18	5.53E+18	3.35E+18	2.68	0.06	430.04	92.27	9.3
84	220	2005-07-13 18:10	2005-07-20 01:55	1.65E+12	1.18E+13	1.02	0.19	1.05E+19	1.05E+19	2.82E+18	7.01	1.25	443.63	53.29	1.56
85	221	2005-07-26 23:20	2005-08-04 21:40	3.09E+06	3.65E+07	0.49	0.83	3.17E+20	3.17E+20	1.61E+20	4.39	1.58	489.66	78.23	2.94
86	224	2006-12-05 17:35	2006-12-11 08:00	2.08E+06	3.13E+05	2.13	0.31	4.33E+18	4.33E+18	3.23E+18	3.45	0.03	585.02	90.67	12.46
87	227	2011-03-07 23:15	2011-03-12 07:20	1.00E+09	6.67E+09	0.81	0.27	3.94E+19	3.94E+19	1.56E+19	5.64	1.11	438.2	100.95	4.95
88	229	2011-06-05 20:05	2011-06-12 05:30	4.62E+04	4.18E+04	0.89	0.21	5.40E+19	5.40E+19	2.38E+19	2.96	0.14	438	39.49	9.24
89	231	2011-08-09 08:00	2011-08-10 16:20	4.42E+04	5.37E+04	0.85	0.17	3.71E+19	3.71E+19	1.42E+19	3	0.19	449.37	77.31	13.15
90	232	2011-09-06 23:45	2011-09-08 13:35	5.64E+02	1.31E+02	2.01	0.36	3.55E+18	3.55E+18	3.21E+18	2.51	0.05	491.28	106.18	10.22
91	236	2011-11-26 09:00	2011-11-30 00:20	2.42E+06	9.56E+05	2.33	0.5	4.18E+18	4.18E+18	4.45E+18	4.7	0.1	415.88	39.84	7.18
92	237	2012-01-26 11:25	2012-02-03 03:55	2.30E+05	2.05E+04	4.57	0.75	7.87E+15	7.87E+15	1.41E+15	3.1	0.02	437.29	93.44	13.06
93	239	2012-03-05 00:30	2012-03-17 02:25	6.75E+06	8.57E+05	1.8	0.34	1.70E+19	1.70E+19	1.43E+19	3.48	0.02	491.29	115.42	2.13
94	240	2012-05-17 02:05	2012-05-20 15:15	1.64E+05	2.17E+05	0.56	0.18	1.67E+20	1.67E+20	6.56E+19	2.8	0.16	417.18	84.53	15.84
95	244	2012-07-12 18:05	2012-07-13 13:00	1.40E+06	3.75E+05	4.32	0.58	1.10E+16	1.10E+16	1.53E+16	4.48	0.07	443.89	84.35	12.58
96	247	2012-09-28 01:20	2012-10-01 03:35	1.90E+05	1.02E+05	2.6	0.35	2.15E+17	2.15E+17	3.23E+17	3.98	0.13	324.32	30.3	2.9
97	250	2013-04-11 09:25	2013-04-14 17:00	4.23E+04	7.50E+03	2.56	0.36	8.32E+17	8.32E+17	7.44E+17	3.13	0.04	406.66	55.84	12.57
98	251	2013-05-14 07:20	2013-05-21 15:20	2.98E+05	7.13E+04	3.12	0.8	1.07E+18	1.07E+18	1.80E+18	4.23	0.06	388.82	24.88	3.12
99	252	2013-05-22 13:45	2013-05-25 23:35	8.41E+06	1.28E+06	4.72	0.62	3.17E+15	3.17E+15	4.83E+15	4.12	0.03	574.21	110.62	33.82
100	260	2015-06-18 05:05	2015-07-02 17:05	9.13E+08	2.41E+08	3.33	0.42	3.41E+17	3.41E+17	3.31E+17	5.99	0.07	447.6	139.7	10.58
101	261	2016-01-02 01:05	2016-01-03 12:55	3.31E+04	6.53E+03	3.85	1.85	4.83E+17	4.83E+17	1.82E+17	3.75	0.05	489.53	61.4	10.46
102	262	2017-07-14 04:50	2017-07-15 00:00	5.16E+04	1.24E+04	3.04	1.1	1.78E+18	1.78E+18	4.10E+18	3.84	0.06	437.96	87.08	2.17
103	263	2017-09-04 22:30	2017-09-15 12:40	1.07E+15	3.09E+16	0.24	0.12	1.32E+20	1.32E+20	5.85E+19	5.03	2.04	560.26	94.12	7.84

[1] Number in SEPEM reference event list.

[2] The normalization coefficient for Equation 9 and its uncertainty are expressed in units of $[\#/cm^2/s/sr/MeV]$.

[3] The normalized diffusion coefficient for Equation 9 which is calculated using a constant solar wind speed of 450 $[km/s]$. Expressed in units of $[cm^2/s]$.

[4] The normalized diffusion coefficient for Equation 9 which is calculated using a real-time solar wind speed list in this table. Expressed in units of $[cm^2/s]$.

[5] The real-time solar wind speed for Equation 9 and its uncertainty are expressed in units of $[km/s]$.

Table 4. Integral fluence spectral parameters fitted for 164 events.

No.[1]	No.	Start Time	End Time	C[2]	γ_1	γ_2	E_0[3]	E_{break}[4]	C_err[2]	γ_1_err	γ_2_err	E_0_err[3]	E_{break}_err[4]	GLE[4]	flare	χ^2
1	2	1974-07-03 01:00	1974-07-10 13:30	4.62E+09	-2.3	-5.57	9.44	30.85	1.33E+09	0.18	0.08	1.05	7.51			31.24
2	3	1974-09-11 00:00	1974-10-03 18:00	1.98E+09	-2.04	-3.5	8.94	13.1	1.93E+09	0.83	0.02	7.18	33.43			23.20
3	4	1974-11-05 07:00	1974-11-08 19:00	2.13E+07	-2.21	-2.98	52.04	39.76	4.44E+06	0.12	0.03	16.83	66.78			1.03
4	5	1975-08-21 17:00	1975-08-24 05:00	3.34E+06	-2.06	-3.61	57.53	89.03	4.42E+05	0.06	0.07	6.53	31.15			5.09
5	6	1976-04-30 22:00	1976-05-05 03:30	5.78E+07	-1.95	-2.95	116.25	116.12	6.61E+06	0.05	0.09	16.8	67.22	Yes	X2	2.29
6	7	1976-08-22 16:30	1976-08-24 23:00	4.50E+06	-1.89	-3.89	19.36	38.79	1.03E+06	0.13	0.08	2.71	13.71		M3	18.03
7	9	1977-09-18 16:30	1977-09-23 07:30	4.78E+08	-1.93	-3.32	32.79	45.45	9.03E+07	0.1	0.04	5.4	23.08	Yes	X2	1.62
8	11	1977-11-22 11:00	1977-11-28 13:30	6.13E+07	-1.23	-3.12	27.8	52.3	1.05E+07	0.09	0.04	3	11.64	Yes	X1	1.83
9	12	1978-01-02 07:30	1978-01-06 16:00	7.58E+06	-1.89	-3.74	22.16	40.95	1.90E+06	0.14	0.04	3.39	16.15		C7	22.45
10	14	1978-02-13 08:00	1978-02-22 21:30	1.76E+10	-2.67	-4.46	13.26	23.78	6.17E+09	0.24	0.04	3.23	18.83		M7	43.40
11	15	1978-04-08 04:00	1978-04-16 03:00	6.49E+07	-1.85	-3.48	29.86	48.62	1.23E+07	0.1	0.04	4.08	18.09		X2	3.13
12	16	1978-04-17 03:30	1978-05-05 02:30	1.14E+10	-2.37	-3.74	14.18	19.43	5.21E+09	0.33	0.03	5.69	28.06	Yes	X5	16.67
13	21	1978-09-23 11:30	1978-10-16 01:30	4.32E+09	-1.76	-3.77	13.22	26.53	1.29E+09	0.19	0.03	2.37	11.31		X1	16.71
14	24	1979-02-17 16:30	1979-02-23 08:00	1.40E+07	-1.77	-3.28	23.7	35.85	3.37E+06	0.14	0.03	4.31	18.07		X2	4.37
15	27	1979-06-06 12:30	1979-06-14 10:00	3.84E+10	-3.57	-6.83	8.02	26.15	1.24E+10	0.21	0.14	1.02	9.35		X2	21.14
16	29	1979-08-01 11:30	1979-09-01 08:00	2.30E+09	-2.36	-3.48	26.95	30.19	6.20E+08	0.17	0.03	7.8	35.85	Yes	X6	5.66
17	30	1979-09-08 12:00	1979-10-03 04:30	1.83E+08	-1.51	-3.76	19.02	42.78	3.69E+07	0.11	0.04	2.04	9.56		X2	4.40
18	31	1979-11-16 00:00	1979-11-23 12:00	9.97E+08	-2.96	-4.44	10.78	15.96	6.20E+08	0.49	0.03	5.48	32.55		M1	36.32
19	34	1980-02-05 18:30	1980-02-09 18:30	6.79E+06	-1.66	-4.19	12.81	32.42	1.85E+06	0.16	0.04	1.65	8.67		M3	32.65
20	35	1980-03-29 19:30	1980-04-08 20:00	3.01E+06	-1.59	-3.15	30.92	48.31	5.98E+05	0.1	0.04	4.58	18.33		C5	4.26
21	36	1980-07-17 15:30	1980-07-26 18:30	5.92E+09	-2.96	-6.72	7.1	26.72	1.91E+09	0.21	0.16	0.8	7.22		M3.4	25.99
22	39	1980-10-15 10:30	1980-10-24 16:30	7.76E+07	-1.89	-5.44	8.59	30.45	2.27E+07	0.18	0.16	0.91	6.71		M2.1	10.58
23	40	1980-11-09 02:00	1980-12-05 08:30	9.31E+07	-2.36	-11.29	11.38	101.68	1.96E+07	0.12	2.15	0.74	32.67		M7.2	106.87
24	41	1981-03-26 03:30	1981-04-07 20:30	1.43E+08	-2.59	-3.02	202.65	88.35	2.09E+07	0.07	0.07	83.3	345.35		M3.5	5.90
25	42	1981-04-24 04:00	1981-04-26 11:00	1.19E+08	-1.33	-3.61	13.14	30	3.43E+07	0.18	0.04	2.03	9.16	Yes	X5.9	34.01

Table 4 *continued on next page*

Table 4 *(continued)*

No.	No.[1]	Start Time	End Time	C[2]	γ_1	γ_2	E_0[3]	E_{break}[4]	C_err[2]	γ_1_err	γ_2_err	E_0_err[3]	E_{break}_err[4]	GLE	flare	χ^2
26	43	1981-07-20 15:00	1981-07-28 07:00	3.79E+08	-2.51	-3.61	33.73	36.92	8.53E+07	0.13	0.04	8.17	38.96		M5.4	6.51
27	48	1981-10-08 03:30	1981-10-26 22:30	3.35E+09	-2.04	-3.46	31.28	44.24	6.75E+08	0.11	0.04	5.27	23.54	Yes	X3.6	4.71
28	51	1981-12-05 17:00	1981-12-14 08:00	1.80E+09	-3.18	-5.04	15.95	29.6	5.33E+08	0.19	0.14	3.28	22.39		M5.2	3.34
29	53	1982-01-29 19:00	1982-02-12 01:00	1.81E+09	-1.69	-4.3	11.26	29.41	5.14E+08	0.18	0.04	1.51	8.13		X1.1	29.49
30	54	1982-03-07 06:30	1982-03-10 08:30	4.04E+07	-2.43	-3.37	20.3	19.13	1.92E+07	0.34	0.03	12.07	54.61			12.12
31	56	1982-06-03 00:00	1982-07-02 06:00	9.82E+07	-1.98	-3.65	18.16	30.19	2.80E+07	0.18	0.04	3.81	17.88		X12	33.11
32	57	1982-07-09 02:30	1982-07-27 05:00	6.21E+10	-3.23	-5.04	11.16	20.24	2.73E+10	0.32	0.04	3.37	22.43		X9	69.02
33	60	1982-12-25 20:00	1983-01-10 00:30	3.52E+09	-2.68	-4.71	11.77	23.9	1.23E+09	0.24	0.04	2.54	15.52		X2.2	53.49
34	61	1983-02-03 08:30	1983-02-10 04:00	1.97E+10	-3.99	-5.26	21.66	27.49	6.14E+09	0.2	0.05	6.62	46.89		X4.1	73.02
35	63	1983-06-14 18:00	1983-06-29 15:00	5.41E+06	-1.47	-3.72	27.14	61.09	9.35E+05	0.09	0.04	2.46	11.35		C2.6	5.31
36	66	1984-03-07 01:00	1984-03-23 07:00	9.56E+07	-2.43	-5.11	134.7	361.03	6.42E+07	0.02	0.16	6.57	54.9		M2	29.19
37	67	1984-04-25 09:30	1984-05-15 19:30	2.58E+09	-2.07	-4.5	23.66	57.42	1.14E+08	0.03	2.07	1.6	50.09		X13	5781.59
38	69	1985-01-22 02:30	1985-01-25 18:00	1.59E+07	-2.37	-3.98	56.09	90.79	2.23E+06	0.06	0.14	6.46	36.2		X4.7	9.39
39	71	1985-07-09 02:30	1985-07-12 13:30	7.95E+06	-1.49	-3.72	19.05	42.48	1.63E+06	0.11	0.03	2.12	9.77		M2.9	9.77
40	73	1986-02-14 10:55	1986-02-19 07:40	1.30E+08	-1.31	-3.79	9.35	23.24	4.62E+07	0.24	0.02	1.59	7.49		M6.4	14.74
41	75	1986-05-04 12:20	1986-05-05 13:15	1.04E+06	-1.23	-4.56	18.12	60.39	1.72E+05	0.08	0.08	1.16	6.86		M1.2	10.83
42	76	1987-11-07 22:45	1987-11-10 13:15	2.37E+08	-2.16	-6.33	9.56	39.93	5.37E+07	0.13	0.16	0.7	6.19		M1.2	22.20
43	77	1987-12-30 02:15	1988-01-01 02:05	4.69E+07	-2.22	-3.83	9.49	15.29	3.36E+07	0.58	0.09	5.3	26.97		C1.7	0.04
44	78	1988-01-02 23:00	1988-01-06 13:50	6.52E+08	-2.43	-5.27	17.82	50.66	1.20E+08	0.1	0.17	1.52	11.35		X1.4	0.40
45	80	1988-11-08 15:45	1988-11-10 11:40	2.74E+06	-1.58	-3	31.06	44.15	5.26E+05	0.11	0.04	5.24	20.03		M3	16.81
46	83	1989-03-08 03:30	1989-03-14 19:50	1.09E+10	-2.73	-4.92	14.76	32.2	2.89E+09	0.16	0.04	2.18	13.78		X15	49.58
47	84	1989-03-23 20:15	1989-03-24 21:30	2.86E+07	-2.14	-4.69	21.4	54.58	4.87E+06	0.09	0.04	1.7	9.98		X1.5	16.92
48	85	1989-04-10 21:15	1989-04-18 01:45	1.01E+09	-1.91	-6.29	8.29	36.23	2.42E+08	0.14	0.12	0.58	4.82		X3.5	9.20
49	87	1989-05-24 05:00	1989-05-29 10:00	4.00E+07	-1.52	-7.37	6.89	40.3	1.08E+07	0.16	0.37	0.52	6.43		M5.7	74.86
50	89	1989-07-25 09:05	1989-07-26 17:45	1.50E+06	-1.17	-2.56	51.3	71.25	3.60E+05	0.11	0.02	9.25	29.34	Yes	X2.6	9.67
51	90	1989-08-12 15:45	1989-08-15 15:45	1.96E+08	-0.25	-4.52	9.64	41.11	4.12E+07	0.12	0.02	0.55	2.85	Yes	X2.6	33.06
52	91	1989-09-12 13:30	1989-09-16 01:30	6.43E+07	-1.85	-5.89	11.73	47.44	1.28E+07	0.11	0.16	0.75	6.31		M5.3	2.51

Table 4 *continued on next page*

WANG & GUO

Table 4 (continued)

No.	No.[1]	Start Time	End Time	C[2]	γ1	γ2	E0[3]	Ebreak[4]	C_err[2]	γ1_err	γ2_err	E0_err[3]	Ebreak_err[4]	GLE	flare	χ2
53	92	1989-09-29 11:55	1989-10-10 05:20	3.42E+08	-0.99	-2.83	24.53	44.95	6.32E+07	0.1	0.02	2.93	10.04	Yes	X9.8	3.79
54	93	1989-10-19 13:10	1989-11-09 16:50	9.14E+09	-1.35	-2.89	13.2	20.35	3.90E+09	0.3	0.02	4.26	15.74	Yes	X13	7.21
55	94	1989-11-15 07:25	1989-11-16 11:45	6.45E+06	-1.92	-3.78	328.25	608.35	3.82E+05	0.02	0.43	19.94	203.04	Yes	X3.2	10.21
56	95	1989-11-27 06:25	1989-12-05 09:05	5.86E+08	-0.3	-5.07	4.58	21.87	2.34E+08	0.28	0.02	0.46	2.76		X2.6	80.62
57	96	1990-03-19 06:30	1990-03-22 01:40	6.23E+08	-1.26	-7.1	8.23	48.12	9.05E+07	0.11	0.94	0.67	10.6		X1	231.21
58	99	1990-04-16 06:05	1990-04-23 07:15	1.89E+08	-2.26	-5.15	14.94	43.14	4.02E+07	0.12	0.15	1.45	10.31		X1.5	9.23
59	100	1990-04-28 05:30	1990-04-29 16:40	4.65E+07	-1.33	-5.38	10.63	43.04	9.74E+06	0.12	0.12	0.74	5.35		C1.2	1.04
60	102	1990-05-17 21:30	1990-05-24 19:00	1.22E+08	-1.98	-2.78	90.48	71.72	1.68E+07	0.07	0.02	18.41	66.98	Yes	X5.5	3.98
61	105	1990-07-26 04:20	1990-07-30 01:35	9.48E+08	-3.15	-3.89	55.55	41.08	2.02E+08	0.12	0.04	19.49	102.6		M2.3	31.68
62	106	1990-07-31 15:25	1990-08-06 12:05	6.18E+08	-2.01	-5.35	11.67	38.9	1.36E+08	0.13	0.1	0.96	6.69		M4.4	0.06
63	108	1991-01-27 14:45	1991-02-02 19:30	1.52E+09	-2.3	-5.81	7.29	25.61	4.80E+08	0.21	0.06	0.82	6.02		X1.3	10.45
64	109	1991-02-08 09:55	1991-02-09 17:05	2.99E+07	-1.98	-6.88	7.93	38.86	6.98E+06	0.14	0.21	0.56	5.61			42.07
65	110	1991-02-25 10:40	1991-02-27 01:55	8.08E+06	-1.53	-5.39	8.25	31.82	2.28E+06	0.18	0.12	0.85	6		X1.2	101.56
66	111	1991-03-12 18:50	1991-03-13 22:25	1.66E+06	-0.91	-5.36	8.77	39.1	3.77E+05	0.13	0.14	0.58	4.3			15.14
67	113	1991-03-23 06:40	1991-03-31 14:30	5.97E+08	-0.29	-4.29	7.58	30.29	1.72E+08	0.18	0.03	0.65	3.25		X9.4	56.71
68	114	1991-04-02 06:45	1991-04-10 01:15	1.17E+09	-2.63	-5.42	14.39	40.28	2.61E+08	0.13	0.13	1.48	10.84		M6	8.28
69	115	1991-04-22 12:00	1991-04-24 15:00	1.62E+07	-2.03	-6.58	12.33	56.08	3.84E+06	0.14	0.23	1.27	11.68			111.89
70	116	1991-05-10 15:05	1991-05-15 10:50	3.65E+08	-2.23	-3.91	32.3	54.29	5.79E+07	0.08	0.02	3.56	17.63		M8.2	24.48
71	118	1991-06-09 19:10	1991-06-15 01:30	1.73E+09	-1.97	-3.71	45.87	80.01	2.36E+08	0.06	0.02	4.07	18.95	Yes	X12	5.14
72	119	1991-06-29 21:25	1991-07-13 05:40	1.05E+10	-1.97	-5.24	7.09	23.19	3.86E+09	0.25	0.03	0.94	6.16		X1.9	59.03
73	120	1991-08-25 21:10	1991-08-30 22:30	3.70E+09	-2.76	-6.25	11.52	40.25	8.20E+08	0.13	0.13	0.94	7.94		X2.1	6.81
74	122	1991-09-30 09:40	1991-10-03 15:40	5.67E+08	-3.21	-4.44	33.13	40.94	1.19E+08	0.12	0.03	6.47	37.99		M7.3	47.14
75	124	1991-10-30 07:30	1991-10-31 20:05	7.33E+06	-1.54	-2.73	48.42	57.28	1.04E+06	0.07	0.02	7.03	24.24		X2.5	14.75
76	126	1991-12-29 05:40	1991-12-30 08:30	5.37E+07	-2.45	-5.03	5.41	13.95	4.83E+07	0.75	0.09	2.37	15.69			2.83
77	127	1992-02-06 22:45	1992-02-10 00:30	1.06E+09	-1.61	-5.43	3.46	13.23	1.04E+09	0.83	0.07	1.09	7.6		M4	0.75
78	128	1992-02-27 11:40	1992-02-28 15:05	1.22E+08	-2.85	-4.15	8.57	11.2	1.72E+08	1.29	0.06	11.42	64.54		C2.6	0.61
79	130	1992-05-09 06:15	1992-05-13 20:15	5.03E+09	-1.84	-5.15	5.98	19.81	2.31E+09	0.33	0.03	0.99	6.41		M7.4	60.54

Table 4 continued on next page

Table 4 (*continued*)

No.	No.[1]	Start Time	End Time	C[2]	γ_1	γ_2	E_0[3]	E_{break}[4]	C_err[2]	γ_1_err	γ_2_err	E_0_err[3]	E_{break}_err[4]	GLE	flare	χ^2
80	131	1992-06-25 20:30	1992-07-01 23:25	4.66E+07	-0.74	-3.19	8.36	20.43	2.02E+07	0.3	0.02	1.73	6.74	Yes	X3.9	24.01
81	132	1992-08-05 20:35	1992-08-08 09:05	3.85E+07	-1.49	-10.07	5.15	44.22	1.16E+07	0.19	0.9	0.36	8.18		M4.8	97.80
82	133	1992-10-30 18:45	1992-11-01 21:20	9.78E+07	-0.32	-5	10.31	48.28	1.64E+07	0.09	0.02	0.44	2.55	Yes	X1.7	41.53
83	134	1993-03-04 13:20	1993-03-05 22:30	5.54E+06	-1.71	-3.68	22.58	44.38	1.09E+06	0.11	0.04	2.8	12.98		C8.1	22.10
84	135	1993-03-06 23:05	1993-03-09 20:10	1.64E+08	-3.06	-4.05	52.96	52.46	3.02E+07	0.1	0.18	11.98	67.66		C1.9	8.50
85	136	1993-03-12 18:50	1993-03-14 15:05	3.84E+07	-2.09	-3.28	33.13	39.39	8.12E+06	0.12	0.03	7.07	30.19		M7	10.02
86	137	1994-02-20 02:20	1994-02-22 21:20	2.14E+08	0.73	-6.7	2.55	18.95	1.04E+08	0.35	0.03	0.2	1.55		M4	30.65
87	138	1994-10-19 22:35	1994-10-21 12:05	1.51E+07	-0.18	-3.73	2.73	9.71	4.44E+07	2.9	0.03	2.84	13.59		M3.2	2.88
88	140	1997-11-06 06:00	1997-11-10 19:40	1.07E+08	-1.47	-3.04	58.41	91.92	1.30E+07	0.05	0.03	5.49	20.77	Yes	X9.4	2.11
89	141	1998-04-20 12:55	1998-04-26 15:05	2.84E+07	-0.19	-5.42	12.56	65.69	4.11E+06	0.09	0.73	0.92	2.71		M1.4	43.89
90	143	1998-05-02 13:55	1998-05-04 23:05	1.33E+07	-1.47	-3.34	57.79	108.07	1.48E+06	0.05	0.03	4.23	17.44	Yes	X1.1	10.79
91	144	1998-05-06 08:25	1998-05-08 00:20	1.53E+07	-1.54	-3.15	28.04	45.04	3.00E+06	0.11	0.03	4.16	16.52	Yes	X2	6.27
92	145	1998-05-09 06:50	1998-05-11 04:10	3.42E+06	-1.38	-4.32	15.56	45.74	7.00E+05	0.11	0.16	1.41	8.59			5.57
93	146	1998-06-17 16:00	1998-06-18 23:55	1.37E+06	-1.03	-3.07	5.02	10.25	2.85E+06	2	0.06	6.42	25.88			0.19
94	147	1998-08-22 17:25	1998-08-31 20:00	2.73E+09	-2.44	-3.85	26.22	36.91	5.92E+08	0.12	0.02	4.64	23.16	Yes	X1	33.13
95	149	1998-09-30 14:25	1998-10-04 04:20	2.94E+08	-1.25	-4.24	9.77	29.22	8.62E+07	0.18	0.03	1.14	5.93		M2.8	29.84
96	152	1998-11-14 06:30	1998-11-17 15:55	1.93E+07	-1.1	-3.73	21.18	55.66	3.15E+06	0.08	0.04	1.62	7.42		C1.7	11.96
97	153	1999-01-21 00:30	1999-01-26 02:40	2.41E+08	-2.86	-4.21	34.39	46.35	4.94E+07	0.11	0.17	6.63	38.87		M5.2	18.65
98	156	1999-05-27 12:15	1999-05-28 14:40	1.31E+06	-1.42	-4.36	15.14	44.47	2.76E+05	0.12	0.16	1.41	8.7			12.42
99	157	1999-06-01 22:10	1999-06-07 15:05	1.50E+08	-1.94	-4.32	17.94	42.8	3.04E+07	0.11	0.04	1.91	10.37		M3.9	40.25
100	158	2000-02-18 08:45	2000-02-19 11:55	1.26E+06	-1.32	-5	18.42	67.72	1.29E+05	0.07	0.31	1.67	6.11		M1.3	65.29
101	161	2000-06-10 04:00	2000-06-12 21:10	3.01E+07	-2	-3.93	31.73	61.15	4.95E+06	0.08	0.05	3.39	17.01		M5.2	19.90
102	163	2000-07-13 00:30	2000-07-23 19:20	2.97E+08	-0.15	-3.63	12.05	41.98	6.15E+07	0.11	0.02	0.84	3.5	Yes	X5.7	8.90
103	164	2000-07-28 02:55	2000-07-30 09:05	7.71E+05	0.07	-10.51	4.36	46.1	2.13E+05	0.17	0.99	0.22	6.51		M1.5	88.37
104	165	2000-08-13 00:45	2000-08-15 03:30	1.05E+09	-3.09	-7.42	3.53	15.29	1.11E+09	0.91	0.83	1.27	13.94			0.00
105	166	2000-09-12 14:50	2000-09-18 01:25	1.70E+09	-2	-4.36	7.2	17.04	5.67E+08	0.28	0.08	1.45	8.13		M1	21.58
106	168	2000-10-25 15:15	2000-10-27 19:10	9.81E+07	-2.38	-5.73	12.38	41.44	2.19E+07	0.13	0.18	1.11	8.95		M2	26.81

Table 4 *continued on next page*

WANG & GUO

Table 4 *(continued)*

No.[1]	No.	Start Time	End Time	C[2]	γ_1	γ_2	E_0[3]	E_{break}[4]	C_err[2]	γ_1_err	γ_2_err	E_0_err[3]	E_{break}_err[4]	GLE	flare	χ^2
107	170	2000-11-08 23:45	2000-11-15 17:00	6.74E+08	-0.87	-5.1	24.26	102.77	7.49E+07	0.05	0.03	0.8	4.82		M7.4	14.95
108	171	2000-11-24 07:00	2000-11-25 20:10	1.04E+08	-2.3	-3.43	41.05	46.58	1.91E+07	0.1	0.04	8.41	37.84		X2	20.94
109	176	2001-04-02 11:20	2001-04-07 08:20	1.70E+08	-1.21	-4.05	15.13	42.96	3.50E+07	0.11	0.04	1.35	6.71	Yes	X20	19.41
110	178	2001-05-07 15:00	2001-05-09 19:10	1.53E+08	-2.31	-5.45	12.14	38.1	3.36E+07	0.13	0.13	1.11	8.14			14.00
111	179	2001-05-20 08:45	2001-05-21 14:25	2.49E+05	-0.8	-2.99	22.84	49.9	2.82E+05	0.51	0.13	10.24	38.24		M6.4	15.69
112	182	2001-08-16 00:55	2001-08-26 04:40	2.69E+07	-1.13	-5.14	38.3	153.78	2.48E+06	0.04	0.04	1.26	7.95			34.27
113	183	2001-09-24 12:00	2001-10-12 03:05	2.91E+09	-1.45	-5.52	21.52	87.64	3.55E+08	0.06	0.03	0.81	5.39		X2.6	38.96
114	184	2001-10-19 04:55	2001-10-28 16:10	1.13E+08	-2.52	-3.01	148.55	73.58	1.82E+07	0.08	0.05	56.48	231.48		X1	15.29
115	185	2001-11-05 16:55	2001-11-12 20:05	8.17E+08	-0.73	-4.8	15.86	64.49	1.20E+08	0.07	0.02	0.67	3.76	Yes	X1	18.94
116	186	2001-11-17 19:55	2001-11-30 13:00	7.58E+08	-0.46	-5.08	7.77	35.84	1.81E+08	0.14	0.03	0.49	2.94		M9.9	59.82
117	188	2001-12-26 05:55	2002-01-09 07:00	1.20E+09	-2.23	-3.45	58	70.41	1.60E+08	0.06	0.02	7.64	33.95	Yes	M7.1	4.59
118	189	2002-01-10 09:55	2002-01-18 18:35	8.55E+08	-2.4	-4.96	15.84	40.58	1.77E+08	0.12	0.12	1.7	11.32		C9	2.62
119	191	2002-04-17 11:30	2002-04-28 13:35	3.81E+08	-1.14	-7.03	23.15	136.35	3.90E+07	0.04	0.05	0.61	5.34	Yes	X1.5	61.07
120	192	2002-05-22 07:50	2002-05-25 00:15	6.17E+09	-3.45	-4.55	44.37	48.82	1.14E+09	0.1	0.16	10.17	64.45		C5	0.24
121	193	2002-07-07 14:00	2002-07-09 13:55	1.67E+06	-0.83	-4.26	11.97	41	3.64E+05	0.12	0.12	0.98	5.6		M1	0.66
122	194	2002-07-16 13:20	2002-07-30 16:30	5.09E+09	-3.05	-4.46	32.46	45.49	1.02E+09	0.11	0.15	6.17	37.93		X3	1.55
123	197	2002-08-22 03:10	2002-08-27 23:10	5.75E+08	-2.22	-3.21	70.74	70.36	7.62E+07	0.06	0.02	11.44	47.89	Yes	X3.1	6.06
124	200	2002-11-09 17:10	2002-11-11 21:15	1.39E+08	-1.31	-4.81	7.65	26.73	4.25E+07	0.2	0.06	0.8	4.81		M4.6	0.46
125	205	2003-10-28 03:30	2003-10-29 16:50	9.35E+08	-0.73	-4.18	15.31	52.8	1.61E+08	0.09	0.02	0.88	4.3	Yes	X17	16.71
126	207	2003-12-02 12:50	2003-12-06 06:05	5.12E+07	-0.63	-9.87	4.41	40.73	1.33E+07	0.15	0.31	0.19	3.15		C7	59.53
127	208	2004-04-11 06:45	2004-04-12 23:05	2.70E+09	-3.51	-5	24.91	37.08	6.08E+08	0.13	0.12	4.98	33.86		C9.6	12.40
128	209	2004-07-23 15:05	2004-07-28 18:10	1.63E+09	-2.29	-5.37	11.27	34.78	4.02E+08	0.15	0.09	1.14	7.96		M1.2	0.57
129	210	2004-07-31 20:55	2004-08-02 14:45	1.27E+06	-0.33	-9.67	4.66	43.55	3.77E+05	0.18	0.76	0.28	6.17			95.19
130	211	2004-09-13 19:55	2004-09-17 18:15	4.49E+09	-2.38	-6.29	7.2	28.15	1.38E+09	0.2	0.08	0.72	5.75		M4.8	11.18
131	213	2004-11-01 06:10	2004-11-02 20:15	1.21E+06	-0.63	-3.69	14.62	44.81	2.35E+05	0.11	0.04	1.17	5.19		M1.1	22.58
132	214	2004-11-07 02:50	2004-11-09 02:45	6.63E+09	-3.09	-6.7	26.75	96.34	7.76E+08	0.06	0.13	1.42	13.72		X2	64.63
133	216	2005-01-20 01:00	2005-01-21 00:00	5.07E+07	-1.01	-2.57	47.53	74.14	6.61E+06	0.06	0.02	4.75	14.88	Yes	X7.1	1.78

Table 4 *continued on next page*

Table 4 (*continued*)

No.	No.[1]	Start Time	End Time	C[2]	γ_1	γ_2	E_0[3]	E_{break}[4]	C_err[2]	γ_1_err	γ_2_err	E_0_err[3]	E_{break}_err[4]	GLE	flare	χ^2
134	218	2005-05-13 21:00	2005-05-17 12:30	9.05E+08	-0.69	-5.78	3.65	18.53	4.69E+08	0.38	0.06	0.44	3.12		M8	15.66
135	219	2005-06-16 20:50	2005-06-18 05:55	1.78E+06	-0.83	-3.21	23.33	55.58	2.85E+05	0.08	0.04	1.92	7.49		M4	6.19
136	220	2005-07-13 18:10	2005-07-20 01:55	1.40E+08	-1.42	-4.74	11.79	39.15	3.06E+07	0.13	0.1	0.98	6.06		M5	0.53
137	221	2005-07-26 23:20	2005-08-04 21:40	7.37E+08	-2.19	-4.64	14.99	36.77	1.71E+08	0.14	0.1	1.76	10.72		M3.7	1.10
138	223	2005-09-07 23:25	2005-09-16 22:55	3.06E+10	-2.97	-5.37	155.41	371.88	2.02E+09	0.02	0.16	8.65	73.09		X17	32.98
139	224	2006-12-05 17:35	2006-12-11 08:00	3.44E+09	-2.07	-4.71	38.62	102.26	3.79E+08	0.05	0.04	2.13	12.46	Yes	X9	38.34
140	226	2010-08-18 08:50	2010-08-19 11:55	4.38E+06	-1.58	-3.63	5.88	12.06	5.04E+06	1.02	0.07	4.03	19.25			7.02
141	227	2011-03-07 23:15	2011-03-12 07:20	1.71E+08	-1.71	-5.04	10.12	33.69	4.36E+07	0.16	0.1	1.01	6.59		M3.7	3.94
142	229	2011-06-05 20:05	2011-06-12 05:30	1.85E+07	-1.41	-3.2	32.25	57.75	3.03E+06	0.08	0.04	3.59	14.36		M2.5	6.82
143	230	2011-08-04 04:35	2011-08-07 11:30	3.06E+08	-2	-3.91	17.11	32.72	7.81E+07	0.15	0.03	2.76	13.74		M9.3	26.21
144	231	2011-08-09 08:00	2011-08-10 16:20	3.04E+06	-1.37	-3.21	29.15	53.64	5.26E+05	0.09	0.04	3.28	13.14		X6.9	11.25
145	232	2011-09-06 23:45	2011-09-08 13:35	6.89E+05	-1.03	-3.74	22.54	61.15	1.11E+05	0.08	0.05	1.72	8.03		C1.4	29.00
146	236	2011-11-26 09:00	2011-11-30 00:20	6.69E+08	-1.96	-5.36	7.47	25.41	2.21E+08	0.22	0.07	0.89	6.07		C1	10.02
147	237	2012-01-26 11:25	2012-02-03 03:55	7.95E+07	-0.66	-4.1	11.91	40.98	1.60E+07	0.11	0.02	0.81	3.9		X1.7	21.52
148	239	2012-03-05 00:30	2012-03-17 02:25	4.22E+09	-1.88	-4.22	42.74	99.9	4.79E+08	0.05	0.03	2.59	13.46		X5.4	16.89
149	240	2012-05-17 02:05	2012-05-20 15:15	1.97E+08	-2.17	-2.91	110.62	81.23	2.58E+07	0.06	0.03	23	88.41	Yes	M5.7	3.99
150	241	2012-05-26 23:55	2012-05-29 04:55	1.59E+07	-0.91	-4.11	4.35	13.89	1.40E+07	0.73	0.08	1.48	7.7		C1.1	2.79
151	242	2012-06-16 09:45	2012-06-17 18:20	4.15E+08	-2.99	-4.34	9.22	12.39	4.49E+08	0.94	0.07	8.95	52.63		M1.9	2.32
152	244	2012-07-12 18:05	2012-07-13 13:00	4.63E+06	-0.04	-5.54	4.67	25.66	1.53E+06	0.22	0.07	0.34	2.33		X1.4	15.33
153	245	2012-07-17 15:50	2012-07-26 18:00	3.20E+08	-1.96	-5.24	25.24	82.86	4.06E+07	0.06	0.09	1.39	9.84		M1.8	47.88
154	247	2012-09-28 01:20	2012-10-01 03:35	9.89E+06	-1.5	-4.33	14.6	41.29	2.16E+06	0.12	0.13	1.47	8.54		C3.7	2.97
155	249	2013-03-15 19:45	2013-03-18 12:55	2.17E+08	-1.84	-9.62	5.41	42.15	6.27E+07	0.18	0.62	0.38	7.01		M1.1	89.54
156	250	2013-04-11 09:25	2013-04-14 17:00	2.84E+07	-1.35	-3.33	18	35.55	6.59E+06	0.14	0.03	2.52	10.42		M6.5	12.72
157	251	2013-05-14 07:20	2013-05-21 15:20	3.67E+08	-1.77	-5.61	8.48	32.58	9.91E+07	0.17	0.11	0.8	5.82		X1.2	13.12
158	252	2013-05-22 13:45	2013-05-25 23:35	9.07E+07	-0.02	-4.21	5.41	22.63	3.53E+07	0.26	0.03	0.59	2.95		M5	40.23
159	255	2014-02-25 10:15	2014-03-05 19:00	1.74E+08	-0.86	-3.54	5.46	14.64	1.30E+08	0.6	0.02	1.8	8.02		X4.9	20.66
160	256	2014-04-18 14:30	2014-04-21 08:55	3.34E+09	-3.11	-4.15	22.61	23.52	1.19E+09	0.24	0.03	9.2	51.28		M7.3	32.65

Table 4 *continued on next page*

Table 4 (continued)

No.	No.[1]	Start Time	End Time	C[2]	γ_1	γ_2	E_0[3]	E_{break}[4]	C_err[2]	γ_1_err	γ_2_err	E_0_err[3]	E_{break}_err[4]	GLE	flare	χ^2
161	260	2015-06-18 05:05	2015-07-02 17:05	5.02E+09	-2	-6.43	6.32	27.98	1.55E+09	0.2	0.09	0.57	4.65		M2	22.17
162	261	2016-01-02 01:05	2016-01-03 12:55	2.68E+08	-3.04	-5	19.83	38.99	5.88E+07	0.13	0.15	3.04	20.84		M2.4	20.94
163	262	2017-07-14 04:50	2017-07-16 13:55	3.36E+08	-2.34	-6.52	9.54	39.84	8.13E+07	0.14	0.24	0.81	7.8		M2.4	46.82
164	263	2017-09-10 05:30	2017-09-15 12:40	4.06E+08	-1.28	-3.56	29.56	67.13	5.92E+08	0.07	0.02	2.25	9.68	Yes	X8	6.83

[1] Number in SEPEM reference event list.

[2] The normalization coefficient for Equation 3 and its uncertainty are expressed in units of $[\#/cm^2/sr/MeV]$.

[3] The E_0 for Equation 3 and its uncertainty are expressed in units of $[MeV]$.

[4] The break-point energy for Equation 3 and its uncertainty are expressed in units of $[MeV]$..

REFERENCES

Anderson, T. W. & Darling, D. A. 1954, Journal of the American statistical association, 49, 765

Band, D., Matteson, J., Ford, L., et al. 1993, The Astrophysical Journal, 413, 281

Belov, A., Kurt, V., Mavromichalaki, H., & Gerontidou, M. 2007, Solar Physics, 246, 457

Chollet, E., Giacalone, J., & Mewaldt, R. 2010, Journal of Geophysical Research: Space Physics, 115

Crosby, N., Heynderickx, D., Jiggens, P., et al. 2015, Space Weather, 13, 406

Decker, R. B. & Vlahos, L. 1986, Astrophysical Journal, Part 1 (ISSN 0004-637X), vol. 306, July 15, 1986, p. 710-729., 306, 710

Desai, M. I., Mason, G. M., Dayeh, M. A., et al. 2016, The Astrophysical Journal, 816, 68

Dierckxsens, M., Tziotziou, K., Dalla, S., et al. 2015, Solar Physics, 290, 841

Emslie, A., Dennis, B., Shih, A., et al. 2012, The Astrophysical Journal, 759, 71

Fiandrini, E., Tomassetti, N., Bertucci, B., et al. 2021, Physical Review D, 104, 023012

Fichtel, C. & McDonald, F. 1967, Annual Review of Astronomy and Astrophysics, 5, 351

Forman, M., Ramaty, R., & Zweibel, E. 1986, Physics of the Sun: Volume II: The Solar Atmosphere, 249

Fu, X., Lu, Q., & Wang, S. 2006, Physics of Plasmas, 13

Gopalswamy, N., Yashiro, S., Krucker, S., Stenborg, G., & Howard, R. A. 2004, Journal of Geophysical Research: Space Physics, 109

Guo, J., Wang, B., Whitman, K., et al. 2024, Advances in Space Research

Hathaway, D. H. 2015, Living reviews in solar physics, 12, 1

Jiggens, P. T., Gabriel, S. B., Heynderickx, D., et al. 2011, in 2011 12th European Conference on Radiation and Its Effects on Components and Systems, 549–564

Jones, F. C. & Ellison, D. C. 1991, Space Science Reviews, 58, 259

Kahler, S. 1982, Journal of Geophysical Research: Space Physics, 87, 3439

Kahler, S., Cliver, E., & Ling, A. 2007, Journal of Atmospheric and Solar-Terrestrial Physics, 69, 43

Klein, K.-L. & Dalla, S. 2017, Space Science Reviews, 212, 1107

Kurt, V., Logachev, I. I., Stolpovskii, V., & Daibog, E. 1981, in International Cosmic Ray Conference, Vol. 3, 69–72

Lario, D., Aran, A., Agueda, N., & Sanahuja, B. 2007, Advances in Space Research, 40, 289

Li, G. & Lee, M. A. 2015, The Astrophysical Journal, 810, 82

Mason, G., Li, G., Cohen, C., et al. 2012, The Astrophysical Journal, 761, 104

Mason, G. M. 2007, Space Science Reviews, 130, 231

McCracken, K., Rao, U., Bukata, R., & Keath, E. 1971, Solar Physics, 18, 100

Mewaldt, R., Looper, M., Cohen, C., et al. 2012, Space Science Reviews, 171

Mewaldt, R. A., Cohen, C. M. S., Labrador, A. W., et al. 2005, Journal of Geophysical Research: Space Physics, 110

Osku Raukunen, Rami Vainio, Allan J. Tylka,, et al. 2018, J. Space Weather Space Clim., 8, A04

Parker, E. N. 1963, New York

Parker, E. N. 1965, Planetary and Space Science, 13, 9

Qin, G., Zhang, M., & Dwyer, J. 2006, Journal of Geophysical Research: Space Physics, 111

Reames, D. V. 1999, Space Science Reviews, 90, 413

Reames, D. V. 2013, Space Science Reviews, 175, 53

SILSO World Data Center. 2006–2022, International Sunspot Number Monthly Bulletin and online catalogue

Song, X., Luo, X., Potgieter, M. S., Liu, X., & Geng, Z. 2021, The Astrophysical Journal Supplement Series, 257, 48

Tylka, A. J. 2001, Journal of Geophysical Research: Space Physics, 106, 25333

Van Hollebeke, Ma Sung, M. 1975, Solar Physics, 41, 189

Vugrin, K. W., Swiler, L. P., Roberts, R. M., Stucky-Mack, N. J., & Sullivan, S. P. 2007, Water Resources Research, 43

Wang, Y. & Qin, G. 2023, The Astrophysical Journal, 954, 81

Yu, F., Kong, X., Guo, F., et al. 2022, The
    Astrophysical Journal Letters, 925, L13

Zhao, L., Zhang, M., & Rassoul, H. K. 2016, The
    Astrophysical Journal, 821, 62